

The Pennsylvania State University

The Graduate School

College of Engineering

**DEVELOPMENT AND VALIDATION OF A FINITE ELEMENT ANALYSIS
MODEL USED TO ANALYZE COUPLING REACTIONS BETWEEN A
TRACTOR'S FIFTHWHEEL AND A SEMITRAILER'S KINGPIN**

A Thesis in

Mechanical Engineering

by

Brent William Shoffner

© 2008 Brent William Shoffner

Submitted in Partial Fulfillment
of the Requirements
for the Degree of

Master of Science

May 2008

The thesis of Brent William Shoffner was reviewed and approved* by the following:

Moustafa El-Gindy
Senior Scientist, Applied Research Laboratory
Thesis Co-Advisor

Kevin Koudela
Research Associate, Applied Research Laboratory
Thesis Co-Advisor

Aman Haque
Assistant Professor of Mechanical Engineering

Karen Thole
Professor of Mechanical Engineering
Head of the Department of Mechanical and Nuclear Engineering

*Signatures are on file in the Graduate School

ABSTRACT

Visual inspections of selected semitrailers during routine equipment checks revealed that the kingpin bent 180 degrees from the direction that the semitrailer is towed. Confirmation from semitrailer repair facilities found that in some cases the semitrailer's supporting structure developed unexpected cracks. These cracks were not thought to be age related but were most likely caused by high stresses from coupling. A literature search found no valid documented kingpin coupling tests and determined the SAE J133 kingpin loading requirements were incorrect. Previous reports relating to kingpin impact testing only tested the kingpin itself and not the kingpin supporting structure on the semitrailer or employed vague descriptions of actual test procedures.

The development of a Finite Element Analysis (FEA) model of the tractor-semitrailer coupling determined that high coupling speeds would overload the kingpin-fifthwheel structure. The FEA model also allowed researchers to determine that a damping system would lower the forces at the semitrailer's kingpin and tractor's fifthwheel interface to an acceptable magnitude equivalent to forces experienced during normal operations. To begin the modeling, the kingpin supporting structure consisted of rigid elements.

Validation of the FEA models was provided through two separate sets of tests. A coupling test was conducted at the Applied Research Laboratory (ARL) at the Pennsylvania State University. The FEA model gave predictions of the tractor deceleration during coupling tests within 33% of the measured decelerations at various impact speeds.

The other set of validation tests was conducted at the Mack Trucks facility in Allentown, Pennsylvania. The FEA model was used to predict tractor CG decelerations for a heavy weight trailer to within 10% of the test data.

The original tractor-semitrailer coupling FEA model was refined to include an elastic kingpin supporting structure. The elastic kingpin supporting structure model was compared to the original rigid kingpin supporting structure model; the elastic simulation was within 3% difference when compared to the original Mack Trucks rigid model. The modified semitrailer model was used to predict standardized SAE J133 vertical and horizontal kingpin coupling loads in order to calculate the stress distribution within the kingpin supporting structure.

The simulations and validation tests provided information to develop a fifthwheel damping system. Preliminary design concepts were simulated using the validated coupling FEA model to provide an optimized set of parameters. The implementation of the translational fifthwheel spring/damper system in the simulation resulted in a considerable reduction of impact force and tractor decelerations. The simulations and measured results have provided enough data to facilitate the detailed design of a damping system prototype.

TABLE OF CONTENTS

LIST OF FIGURES	vii
LIST OF TABLES	x
ACKNOWLEDGEMENTS	xii
Chapter 1 INTRODUCTION.....	1
1.1 Motivation	1
1.2 Problem Overview	1
1.3 Literature Survey	4
1.3.1 Standards Regarding Kingpin and Fifthwheel Loads.....	4
1.3.1.1 SAE Standards.....	4
1.3.1.2 ISO Standard	8
1.3.2 Review of Kingpin/Fifthwheel Coupling Related Research	12
1.3.3 Comparison of Maximum Kingpin Load Definitions	16
1.3.4 Coupling and Docking Simulations Using DADS	18
1.3.4.1 DADS [®] Coupling Simulation	19
1.3.4.2 Validation of the DADS [®] Coupling Model	20
1.3.4.3 DADS [®] Coupling Simulation Results.....	21
1.3.4.4 Investigation of the effect of SFWL.....	22
1.3.4.5 DADS [®] Docking Simulation and Results	23
1.4 Thesis Objectives.....	26
1.5 Thesis Outline.....	26
Chapter 2 DEVELOPMENT OF TRACTOR-SEMITRAILER FEA MODEL	27
2.1 FEA Models of Fifthwheel and Kingpin	27
2.2 ARL Tractor & Single-Axle Semitrailer Model.....	29
2.3 Mack Trucks Tractor & Dual-Axle Semitrailer Model.....	31
Chapter 3 ARL COUPLING TESTS AND MODEL VALIDATION	37
3.1 ARL Measurements.....	37
3.2 ARL Model Validation.....	40
3.3 Preliminary Parametric Analysis of a Fifthwheel Damping System.....	41
Chapter 4 MACK TRUCKS COUPLING TESTS AND MODEL VALIDATION ..	45
4.1 Mack Trucks Measurements.....	45
4.2 Tractor Velocity Measurement Methods.....	47
4.3 Mack Trucks Model Validation.....	50
4.3.1 Tractor Impact Deceleration.....	50

4.3.2 Kingpin Impact Force.....	51
4.4 Analysis of Fifthwheel Damping System.....	52
Chapter 5 ELASTIC KINGPIN SUPPORTING STRUCTURE.....	58
5.1 Model Construction of Elastic Kingpin Supporting Structure	58
5.2 Validation of Elastic Kingpin Supporting Structure Model	64
5.3 Simulations of SAE J133 loads “A” and “E”	66
Chapter 6 CONCLUSIONS AND RECOMMENDATIONS.....	73
6.1 ARL Coupling Tests.....	73
6.2 Mack Trucks Coupling Tests.....	74
6.3 Fifthwheel Damping System Analysis	76
6.4 Elastic Kingpin Supporting Structure Model	77
6.5 Recommendations	78
BIBLIOGRAPHY.....	79

LIST OF FIGURES

Figure 1.1: Selected Tractor-Semitrailer (SI Units).....	3
Figure 1.2: Selected Tractor-Semitrailer (British Units)	3
Figure 1.3: SAE J133 drawing of loads “A” and “B” [2].....	5
Figure 1.4: Correct points of application for loads “A”, “B”, and “E” in SAE J133.....	6
Figure 1.5: Detailed drawing of an upper coupler kingpin from SAE J700 [4]	6
Figure 1.6: Allowable bowing of kingpin supporting structure plate from [4]	7
Figure 1.7: Lifting test on fifthwheel couplings from ISO 8717 [3]	10
Figure 1.8: Application of vertical and horizontal test loads from ISO 8717 [3].....	12
Figure 1.9: (a) 6-axle tractor-semitrailer [6] and (b) tractor-semitrailer selected for this report	17
Figure 1.10: Five-axle tractor-semitrailer DADS [®] model [1]	19
Figure 1.11: Coupling Model.....	19
Figure 1.12: Tractor Deceleration vs. Coupling Impact Speed [1].....	21
Figure 1.13: Kingpin Force vs. Coupling Impact Speed [1].....	22
Figure 1.14: DADS Docking Simulation Model [1].....	24
Figure 1.15: Tractor Deceleration vs. Docking Speed [1].....	24
Figure 1.16: Longitudinal Kingpin Force vs. Docking Speed [1]	25
Figure 2.1: Kingpin finite element model and photo.....	28
Figure 2.2: Fifthwheel finite element model and photo.....	28
Figure 2.3: FEA model of the coupled fifthwheel and kingpin	29
Figure 2.4: ARL tractor-flatbed semitrailer FEA model	29
Figure 2.5: Top view of ARL tractor model	30
Figure 2.6: Top view of ARL semitrailer model	30

Figure 2.7: Coupled ARL tractor and semitrailer	31
Figure 2.8: Mack Trucks' truck dimensions	32
Figure 2.9: Mack Trucks' Fontaine trailer dimensions.....	32
Figure 2.10: FEA kingpin support structure model and actual support structure	33
Figure 2.11: Mack Trucks' model side view	34
Figure 2.12: Actual and simulated fifthwheel and kingpin near coupling position....	34
Figure 2.13: Bottom view of Mack Trucks' trailer model.....	35
Figure 2.14: Full isometric view of Mack Trucks' simulated test tractor- semitrailer	35
Figure 3.1: Vertical and longitudinal accelerometers on the ARL tractor (left) and semitrailer (right).....	38
Figure 3.2: ARL low speed tachometer driveline measurement system	39
Figure 3.3: Digital display inside the tractor cab for low speed measurements	39
Figure 3.4: Validation comparison between ARL experimental measurements and FEA simulations	40
Figure 3.5: Bracket displacement of selected damping system parameters.....	42
Figure 3.6: Tractor deceleration of selected damping system parameters.....	42
Figure 3.7: Kingpin impact force of selected damping system parameters.....	43
Table 3.2: Effect of semitrailer weight on coupling dynamics	44
Figure 4.1: Tractor accelerometer on Mack Trucks' instrumented tractor chassis.....	46
Figure 4.2: Trailer accelerometer on Mack Trucks' instrumented Fontaine trailer....	46
Figure 4.3: Digital video frames used for impact speed estimation	47
Figure 4.4: Tractor deceleration vs. impact speed (GPS and digital video) during Mack Trucks' coupling tests.....	49
Figure 4.5: Mack Trucks simulated and measured tractor deceleration vs. impact speed (GPS)	51
Figure 4.6: Mack Trucks measured and simulated impact force vs. impact speed	52

Figure 4.7: Coupling impact forces	54
Figure 4.8: Coupling tractor decelerations.....	55
Figure 4.9: Bracket displacement during heavyweight semitrailer coupling	57
Figure 4.10: Bracket displacement during lightweight semitrailer coupling.....	57
Figure 5.1: Entire side view of elastic kingpin structure model	59
Figure 5.2: Bottom isometric view of semitrailer.....	60
Figure 5.3: Bottom view of bolster plate	61
Figure 5.4: Labeled isometric top view of the kingpin and support structure	62
Figure 5.5: Isometric top view of kingpin supporting structure with weld points.....	63
Figure 5.6: Cut-away view of the kingpin support structure and weld points.....	64
Figure 5.7: Kingpin impact force vs. impact speed for validation of elastic model ...	65
Figure 5.8: Tractor deceleration vs. impact speed for validation of elastic model	66
Figure 5.9: Isometric view of current SAE J133 load “A” Von Mises stress plot	67
Figure 5.10: Side view of current SAE J133 Load “A” Von Mises stress plot.....	68
Figure 5.11: Isometric view of corrected SAE J133 load “A” Von Mises stress plot.....	69
Figure 5.12: Side view of corrected SAE J133 load “A” Von Mises stress plot.....	69
Figure 5.13: Isometric view of Von Mises stress plot from the downward load “E”	70
Figure 5.14: Side view of Von Mises stress plot from the downward load “E”	71
Figure 5.15: Isometric view of Von Mises stress plot from the upward load “E”	72
Figure 5.16: Side view of Von Mises stress plot from the upward load “E”	72

LIST OF TABLES

Table 1.1: Comparison between the two tractors and semitrailers 17

Table 1.2: Validation of DADS[®] Simulation Model [1] 20

Table 1.3: Comparison between different SFWL values at the impact speed of 3.0
km/hr (1.89 mph) 23

Table 2.1: Weight data of ARL tractor-semitrailer used to conduct coupling tests ... 29

Table 3.1: Weights of ARL tractor and single-axle semitrailer 37

Table 4.1: Weights of Mack Trucks’ tractor and Fontaine semitrailer 45

Table 4.2: Mack Trucks’ experimental measurements 48

Table 4.3: Percent reductions by damping system 56

Table 5.1: Mass properties of tractor and semitrailer 58

Table 5.2: Material parameters used for steel 59

Table 5.3: Thickness of selected parts in FEA model 59

NOMENCLATURE

Symbol	Unit	Description
ARL		Applied Research Laboratory
CAD		Computer Aided Design
CAE		Computer Aided Engineering
D	kN	D-Value
d	N	Static tractor drive axle group load
E_o	N	Maximum allowable longitudinal force on the fifthwheel or kingpin
F_A	N (lbs.)	Fifthwheel lifting force
$F_{h,t}$	N (lbs.)	Horizontal test load
$F_{v,t}$	N (lbs.)	Vertical test load
FEA	N (lbs.)	Finite Element Analysis
G, g	m/s^2	Acceleration due to gravity ($9.81 m/s^2$)
GPS		Global Positioning System
GVW	N (lbs.)	Gross Vehicle Weight
ISO		International Organization of Standards
M_1	N	Gross Vehicle Weight (GVW)
M_0	N	Tractor weight
PSU		Pennsylvania State University
R	tonnes ¹	Total mass of the semitrailer and payload
SAE		Society of Automotive Engineers
SFWL	N (lbs.)	Single Fifthwheel Load
T	tonnes	Tractor mass plus kingpin load divided by G
TVW	N (lbs.)	Total weight of semitrailer including payload
U	tonnes	Vertical kingpin or fifthwheel load divided by G
VDSRC		Vehicle Dynamics and Simulation Research Center

¹ 1 tonne = 1000 kg

ACKNOWLEDGEMENTS

The author would like to express his appreciation to Mr. Mukesh Trivedi and his team from Mack Trucks/Volvo 3P, Dr. Randy Schutt and his team from SAF-Holland, which provided the calibrated fifthwheel and instrumented the test tractor semitrailer in collaboration with Mack Trucks, Mr. Mario A. Scaglione and Jeffrey Rozanski of Naval PHST Center, NSWC Indian Head Detachment Earle, Mr. Steve Fleischut of the Applied Research Laboratory (ARL) of Penn State University, Mr. Wayne Evenson of L3-TITAN, and Mr. Steve Bazow of Strategic Systems Program Office (SSPO) for their help, technical support and directions during the course of this important research project.

The author also expresses his gratitude to the Applied Research Laboratory (ARL) of the Pennsylvania State University and Dr. Dick Stern, director of the E&F Graduate Assistant program.

Chapter 1

INTRODUCTION

The first chapter is an introduction to the work performed in this thesis. The following sections compose this chapter: the motivation for the proposed research, an overview of the problem, a literature survey of related work, description of the research objectives, and an outline of the thesis.

1.1 Motivation

A selected tractor-semitrailer was found to be failing in the kingpin supporting structure. The first sign of failure was a bent kingpin. Visual inspections of the semitrailers during routine equipment checks revealed that the kingpin bent 180 degrees from the direction that the semitrailer is towed. In addition, the kingpin supporting structure was found to develop unexpected cracks. These cracks were not thought to be age related because semitrailers with recent kingpin replacement also developed similar cracks. The likely cause of the cracks was thought to be unknown high kingpin loads. Previous simulation research indicated that the coupling maneuverability was responsible for the highest kingpin loads—the loads of which were close to the maximum strength requirements of the Society of Automotive Engineers (SAE) Recommended Practice J133 [1].

1.2 Problem Overview

The coupling of a tractor's fifthwheel to a semitrailer's kingpin is an adopted joint mechanism. Trucks and semitrailers frequently need to be coupled and uncoupled. A coupling operation involves the tractor moving backwards towards the semitrailer until the semitrailer's kingpin interlocks with the tractor's fifthwheel mechanism. This rigid

coupling creates an impact force. Since this coupling is the only method used to connect the tractor and semitrailer, it is necessary for the kingpin and fifthwheel to meet various requirements such as optimal position, installation practices, maintenance intervals, material strength, and fatigue strength.

For these performance requirements, the SAE Recommended Practice J133 specifies test procedures and minimum performance standards for the kingpin and supporting structures [2]; however, the standard incorrectly applies the longitudinal load, and the test procedure defined is conducted using a test fixture, not the actual kingpin. The International Organization for Standardization (ISO) standard 8717 also specifies the test conditions and strength requirements for the fifthwheel coupling [3]. ISO 8717 introduces a comparative value, called the D-value, which can be used as a kingpin and fifthwheel selection index.

The configurations of the selected tractor-semitrailer are specified in Figure 1.1 and Figure 1.2. The weight of each axle is not shown in the figures. The weight of each trailer axle is 6,909.4 N (1,553.3 lbs). The tractor's front axle weighs 5,333.4 N (1,199 lb) and the two drive axles weigh 10,461.8 N (2,351.9 lb) each. Using these data, a tractor-semitrailer finite element model was developed and a coupling operation was simulated in order to investigate the forces applied to the kingpin and fifthwheel structures.

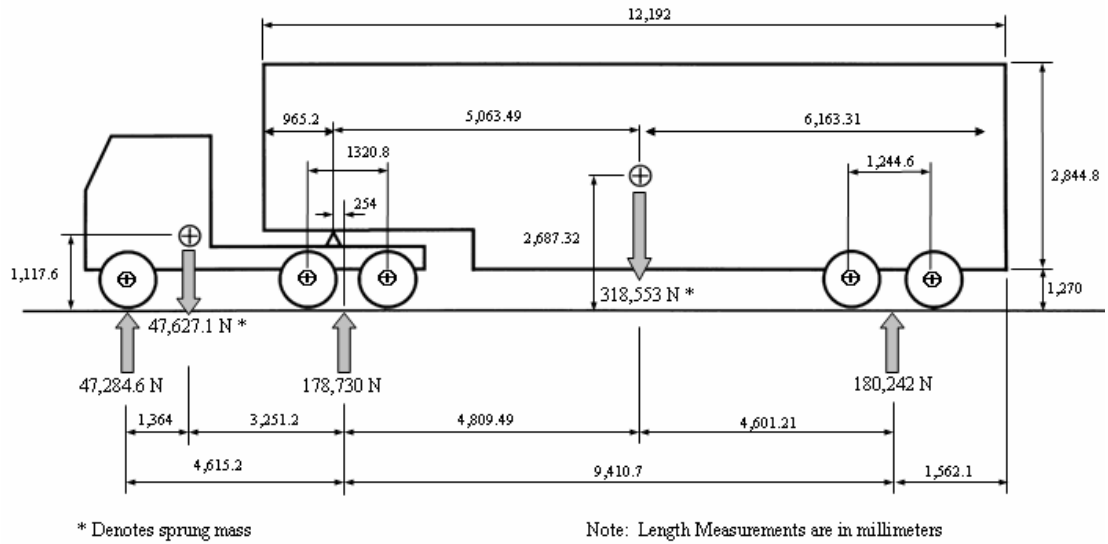


Figure 1.1: Selected Tractor-Semitrailer (SI Units)

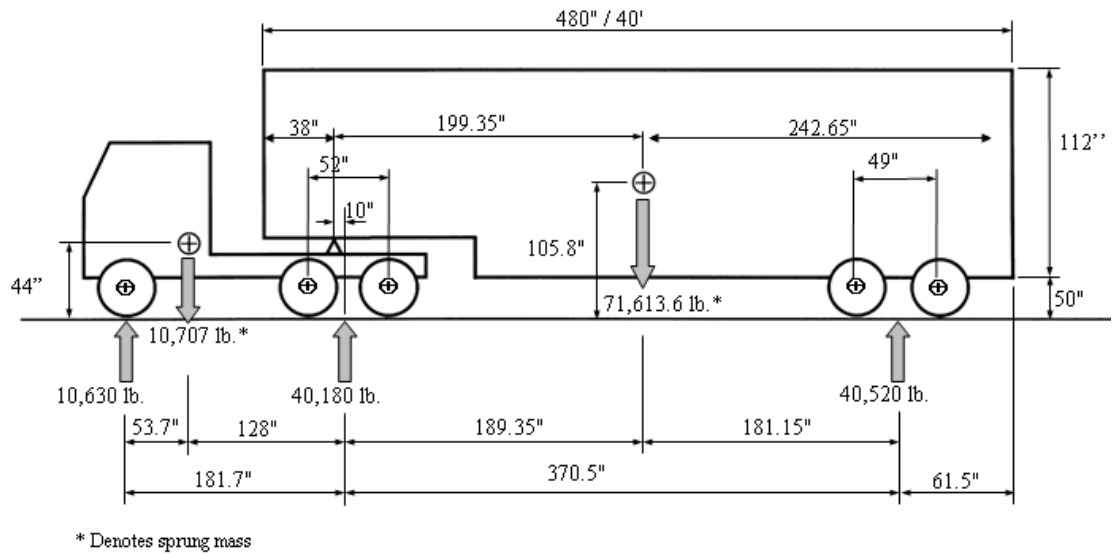


Figure 1.2: Selected Tractor-Semitrailer (British Units)

1.3 Literature Survey

This literature survey presents related work completed in tractor to semitrailer coupling research and development. The literature is presented and discussed to provide insight into previous work completed in modeling and measurement of kingpin operating forces. The literature survey has been split into three sections: kingpin standards, kingpin force modeling, and kingpin force measurements.

1.3.1 Standards Regarding Kingpin and Fifthwheel Loads

Standards from two organizations are reviewed in this section. Two articles are from the Society of Automotive Engineers, and one is from the International Organization for Standardization.

1.3.1.1 SAE Standards

The SAE Recommended Practice J133 [2] was originally established in 1987 to provide test procedures and minimum performance requirements for kingpins and their supporting structures. This standard specifies several single quasi-static forces, fatigue forces, and associated minimum fatigue life cycle counts for the kingpin and its supporting structures. For example, SAE J133 states that the installed kingpin should endure a single force of $1.15 * \text{Trailer weight including payload (TVW)}$ along a fore or aft direction. This single force is denoted as “A” in Figure 1.3. The load “B” in this figure represents a cyclic force of $0.4 * \text{TVW}$ along a fore or aft direction for 500,000 cycles. The test fixture identified in SAE J133 does not test the kingpin, only the test fixture. Some other single and cycling load requirements in horizontal and vertical directions on the kingpin and fifthwheel are also specified in the SAE Standard J133.

These forces (“A” and “B”) can lead to failure of the kingpin base fixation. However, no criteria is given for kingpin selection for a specified trailer weight. With a specific trailer weight, every test in the SAE Practice J133 cannot be performed to check whether the kingpin will meet the expected performance. A method of how to select a kingpin and fifthwheel with a specified gross trailer weight needs to be established.

The kingpin displayed in Figure 1.3 has a 50-mm (2-in) diameter in the neck area, which has been widely adopted. Detailed drawings and dimensions are specified in SAE Standard J700 [4].

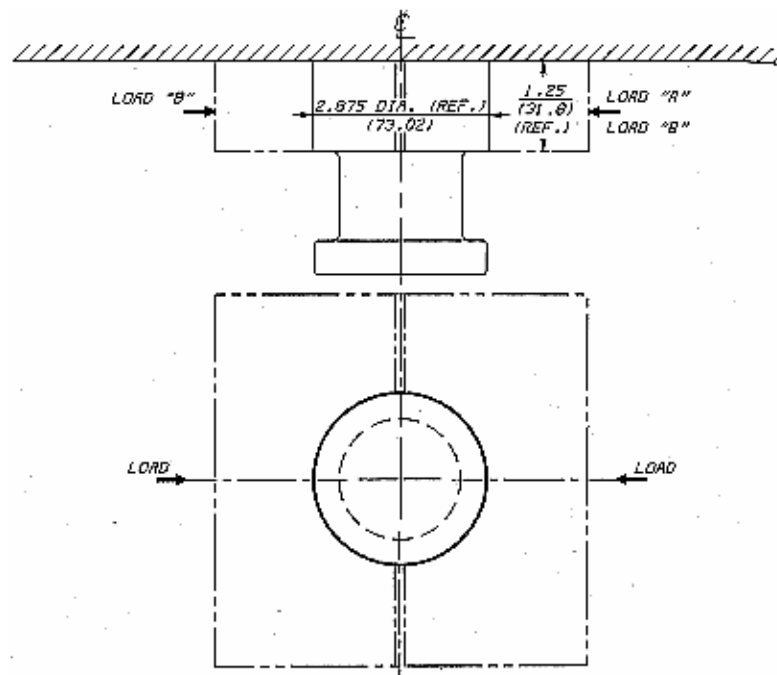


Figure 1.3: SAE J133 drawing of loads “A” and “B” [2]

It should be stated at this point that some details in SAE J133 are vague or incorrect. SAE J133 states that the force “E” is defined as a single application of force of 1.0 * total trailer weight. Therefore, this force “E” is supposed to indicate a specific point for better understanding in the provided SAE J133 figure. The force “E” cannot be found. Also, the points of application for both loads “A” and “B” in Figure 1.3 are incorrect. Loads “A” and “B” should be applied to the 50 mm (2 in.) diameter of the kingpin for a truck’s

fifthwheel. The current placement of load “A” in Figure 1.3 is for “Trailer on Flat Car” operation as specified in Association of American Railroads M931 [5]. The corrected diagram is shown in Figure 1.4. As such, the SAE J133 drawings need to be modified or updated with detailed illustrations.

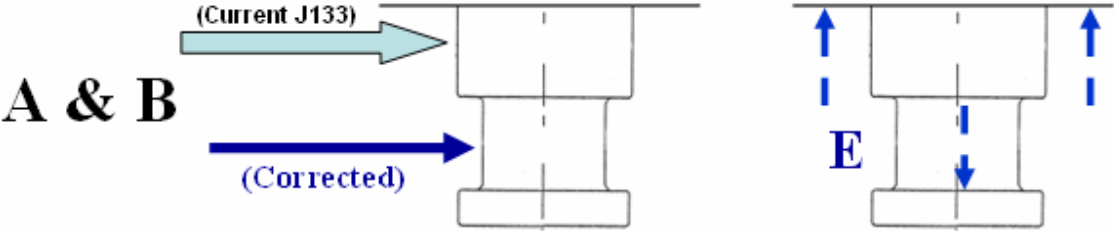


Figure 1.4: Correct points of application for loads “A”, “B”, and “E” in SAE J133

The second SAE Standard is SAE J700 [4]. This standard gives the tolerances and dimensions for the installed kingpin. SAE J700 applies to upper coupler kingpins for commercial trailers and semitrailers in the un-laden condition. The detailed drawing of a kingpin is provided in Figure 1.5. As indicated in Figure 1.6, $90^\circ \pm 1^\circ$ angle extends (in all directions) from the centerline of the kingpin to the upper coupler plate surface within a 48.26 cm (19 in) radius. The units in Figure 1.5 and 1.6 are in millimeters and (inches).

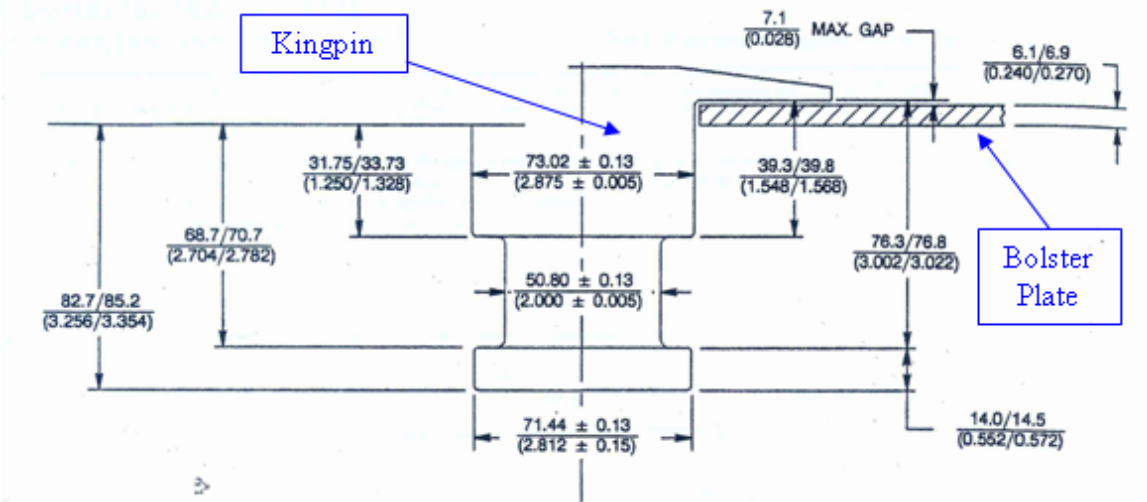


Figure 1.5: Detailed drawing of an upper coupler kingpin from SAE J700 [4]

SAE J700 states that the upper coupler plate surface should not bow downward (convex) more than 0.635 cm (1/4 in) within a 48.26 cm (19 in) radius or more than 0.3175 cm (1/8 in) at a radius of 25.4 cm (10 in) from the kingpin. The upper coupler plate surface should not bow upward (concave) more than 0.15875 cm (1/16 in) within a 48.26 cm (19 in) radius as can be seen in Figure 1.6.

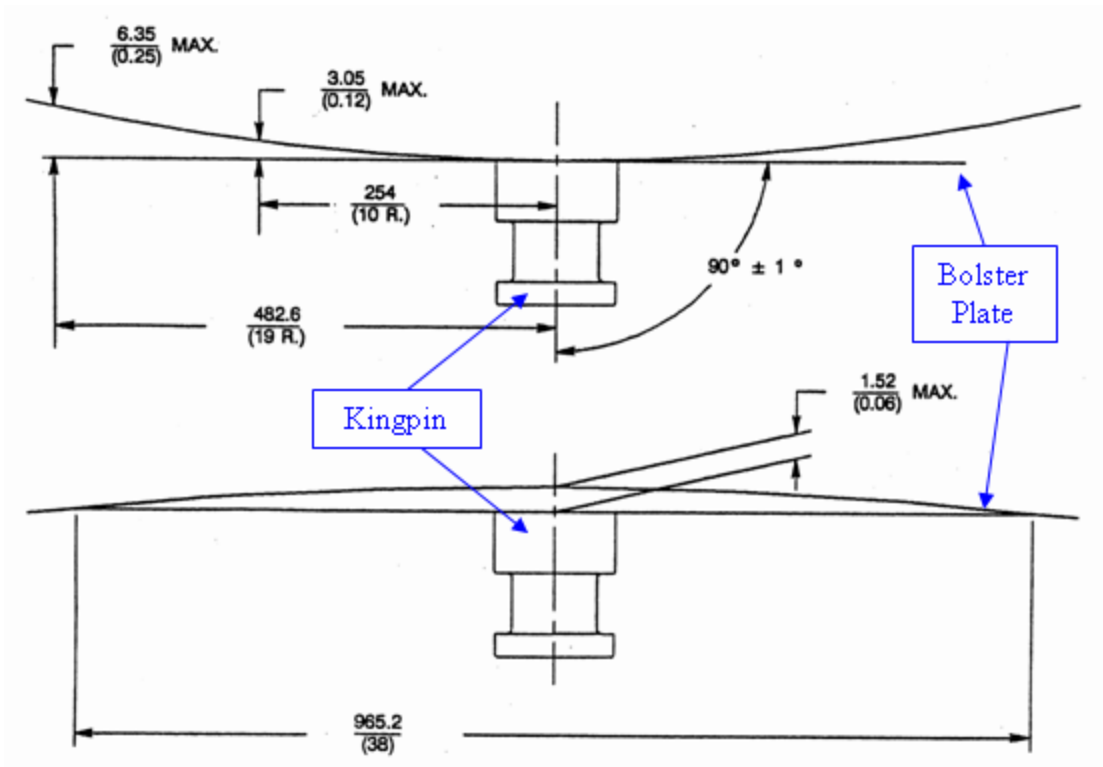


Figure 1.6: Allowable bowing of kingpin supporting structure plate from [4]

In conclusion, the SAE J133 standard mentions several performance requirements on the kingpin and its supporting structure during normal driving maneuvers. The standard contains obscure drawings and little description of the test procedures. Some of the most important findings of the literature survey are the identification of problems found within the published SAE J133. Together, SAE J133 and J700 state that the kingpin, when installed, shall meet the following performance requirements:

1. Withstand a force “A” of $1.15 * \text{Trailer weight including payload (TVW)}$ in a fore or aft direction as shown in Figure 1.3.

2. Withstand a cycling force “B” of $0.4 * TVW$ in a fore and aft direction for 500,000 cycles as shown in Figure 1.3.
3. Withstand a single application of force “E” of “ $1.0 * TVW$ ” up and down through the fixture with the kingpin locked to the plate by its 2.8125 inches (71.44 mm) diameter lip (Figure was missing in SAE J133) [2].
4. Kingpin and supporting structure should withstand these conditions without deformation that will prevent compliance with the installation dimensions of SAE J700 [4].

1.3.1.2 ISO Standard

The ISO Standard 8717 [3] specifies the load requirements and test conditions for semitrailer kingpin to tractor fifthwheel coupling.

In order to specify load requirements, this standard introduces a parameter called the D-value that determines relative longitudinal force occurring between the tractor and semitrailer. This D-value can be also used as an index to select an appropriate kingpin or fifthwheel. In fact, most of the manufacturers of kingpins and fifthwheels provide the D-value with their products. D-value in kN can be determined as follows.

$$D = g \cdot \frac{0.6 \cdot T \cdot R}{T + R - U} \quad \text{Equation 1.1}$$

Where,

T = Tractor mass plus kingpin load divided by g (tonnes),

R = Total mass of the semitrailer and payload (tonnes),

U = Kingpin load divided by g (tonnes),

g = Acceleration due to gravity (9.81 m/s^2).

When tractor mass, semitrailer mass, and vertical kingpin loads are known, the D-value can be calculated with Equation 1.1.

For the selected tractor-semitrailer, the calculated D-value is 111.2 kN. Therefore, a kingpin and a fifthwheel of a higher D-value should be selected to pass the ISO Standard 8717 criterion. The D-value of the kingpin currently in operation on the selected tractor-semitrailer system is 210 kN.

In order to specify test conditions, ISO 8717 states that the fifthwheel coupling shall be equipped with all the mounting hardware necessary to attach it to the vehicle [3]. The method of mounting shall be identical to that employed subsequently on the vehicle itself.

A static lifting test shall be performed on all fifthwheel couplings. When applying a static lifting force of up to F_A shown in Equation 1.2, there shall be no major permanent bending of the coupling plate over more than 0.2 % of its width.

$$F_A = g * U \quad \text{Equation 1.2}$$

Where,

U = Vertical kingpin or fifthwheel load divided by g (tonnes),

g = Acceleration due to gravity (9.81 m/s^2).

The configuration and direction of the lifting force F_A is shown in the test fixture diagram in Figure 1.7. The following circumstances and force calculations are defined in the standard for each specified kingpin diameter:

- In the case of 50 mm (2.0 inch) kingpin and fifthwheel couplings, there shall be no separation of the kingpin from the coupling with a lifting force F_A as calculated in Equation 1.3.

$$F_A = g * 2.5 * U \quad \text{Equation 1.3}$$

- In the case of 90 mm (3.6 inch) kingpin and fifthwheel couplings, there shall be no separation of the kingpin from the coupling with a lifting force F_A as calculated in Equation 1.4.

$$F_A = g * 1.6 * U \text{ (but minimum 500 kN)} \quad \text{Equation 1.4}$$

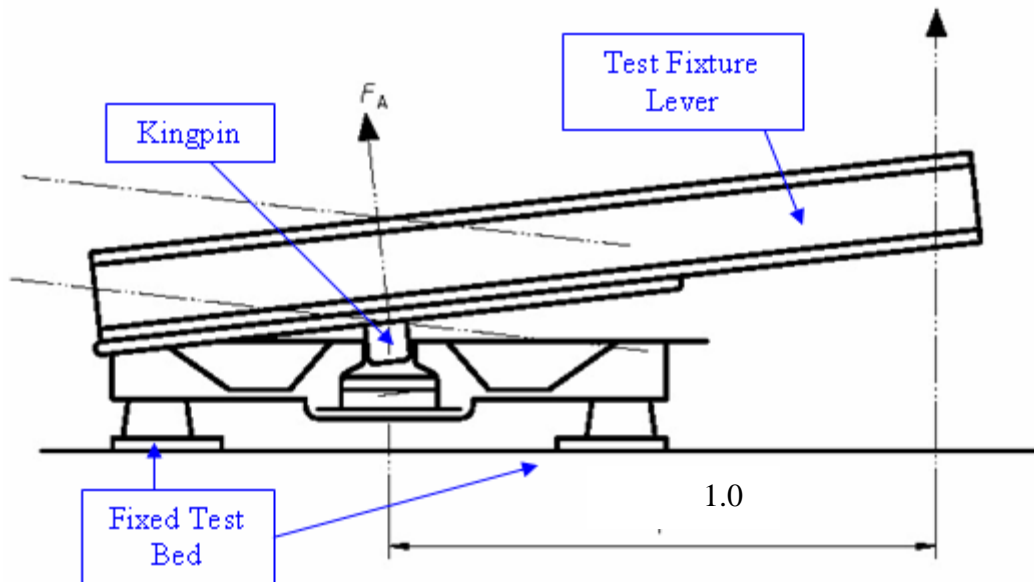


Figure 1.7: Lifting test on fifthwheel couplings from ISO 8717 [3]

The force F_A shall be applied by means of a lever, acting on the coupling plate at one end and raised at the other end at a distance of 1.0 m to 1.5 m from the centre of the kingpin. The lever arm shall be at 90° to the direction of entry of the kingpin into the coupling. If the worst case is obvious, the side of the fifthwheel corresponding to this worst case shall be tested; otherwise, the technical service shall decide which side to test. No second test shall be required.

Dynamic test loads shall be performed on all fifthwheel couplings. Two dynamic loads shall be applied on the fifthwheel that simulate practical loads under driving conditions. The two loads are a vertical test load ($F_{v,t}$) and a horizontal test load ($F_{h,t}$).

The application of these two dynamic loads, $F_{v,t}$ and $F_{h,t}$, are outlined as follows:

- The vertical test load and the horizontal test load shall be applied simultaneously.
- The vertical test load shall be a pulsating force applied in the direction shown in Figure 1.8.

- $F_{v,t}$ shall be applied by means of a rigid counter-plate simulating the semi-trailer skid-plate.
- To ensure constant friction between these plates, suitable measures shall be taken (for example inserting polyamide foil) to guarantee a maximum coefficient of friction, 0.15.
- $F_{v,t}$ shall pulsate between the two values calculated in Equation 1.5.

$$0.4 * U * g < F_{v,t} < 1.2 * U * g \quad \text{Equation 1.5}$$

Where,

U = Kingpin load divided by g (tonnes),

g = Acceleration due to gravity (9.81 m/s^2).

- The horizontal test load shall be an alternating force applied in the direction shown in Figure 1.8.
- $F_{h,t}$ shall be applied by means of a fifthwheel kingpin.
- $F_{h,t}$ shall alternate between the two values calculated in Equation 1.6.

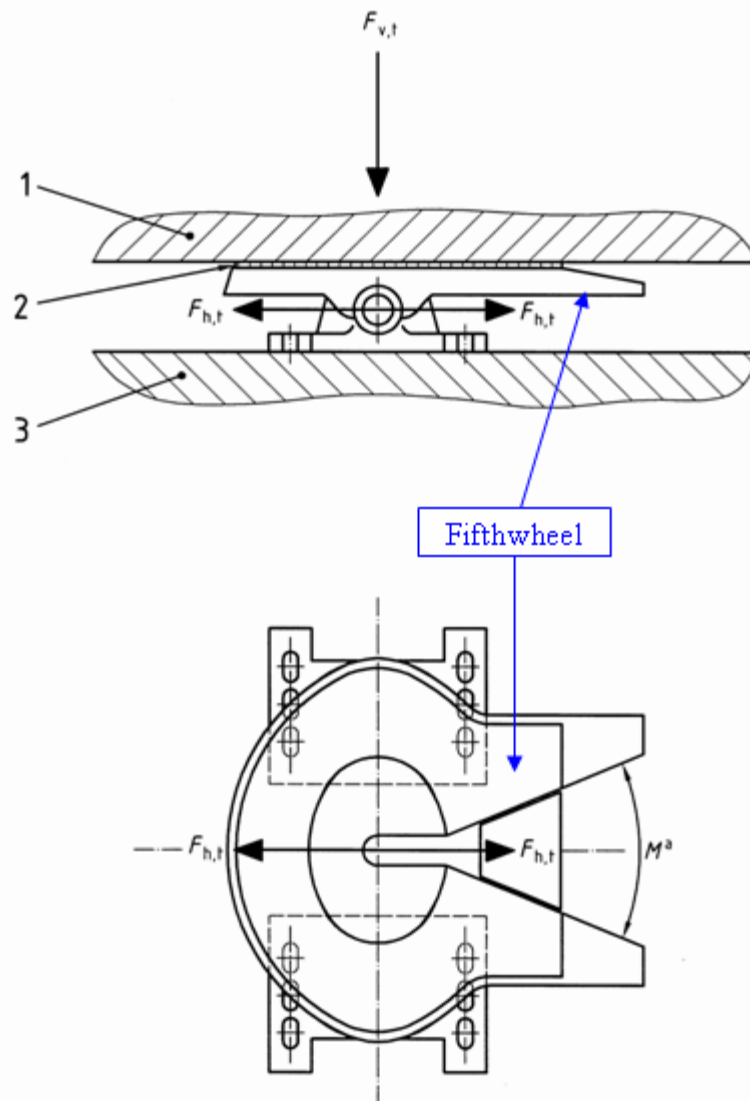
$$-0.6 * D < F_{h,t} < +0.6 * D \quad \text{Equation 1.6}$$

Where,

D is calculated from Equation 1.1.

- The dynamic test shall be carried out sinusoidally and the number of cycles shall be $2 * 10^6$ for each $F_{v,t}$ and $F_{h,t}$ load.
- The selected frequency shall not exceed 35 Hz and shall not coincide with the natural frequency of the system. Since $F_{v,t}$ and $F_{h,t}$ are applied simultaneously, the cycle rates shall differ by 1 % to 3 %.

The strength criteria in ISO 8717 states that the dynamic tests shall not cause permanent deformation, breaks, or cracks. This includes permanent deformation, breaks, or cracks to either the kingpin or the fifthwheel and supporting structures.



1: Counter-plate, 2: Polyamide foil, 3: Test bed

Figure 1.8: Application of vertical and horizontal test loads from ISO 8717 [3]

1.3.2 Review of Kingpin/Fifthwheel Coupling Related Research

Sweatman [6] carried out research to develop strength standards for fifthwheel couplings, turntables, and kingpins used under typical Australian operating conditions. The scope of the research included general transport vehicles (semitrailers) and road trains (multiple

semitrailers to a single tractor). There were currently no effective controls on fifthwheel strength before this research was conducted. In this study, the pin-couplings themselves were already rated according to a valid standard test so it was only necessary to determine the application formulae for vehicle combinations based on the weight of the units.

Sweatman introduced the maximum allowable longitudinal fifthwheel force (E_o) that was formulated by combining the maximum steady state and dynamic forces as shown in Equation 1.7:

$$E_o = \frac{(M_1 - M_0) \cdot (0.7 \cdot M_0 + 0.4 \cdot d)}{M_1} \quad \text{Equation 1.7}$$

Where,

E_o = Maximum allowable longitudinal force on the fifthwheel
or kingpin (N),

M_1 = Gross Vehicle Weight (GVW) (N),

M_0 = Tractor weight (N),

d = Static tractor drive axle group load (N).

In 1970, Teresinski [7] conducted an analysis on a tractor frame/fifthwheel attachment design using a T-section supporting member bolted to a side-rail web. Six different bolt attachment configurations were analyzed for bolt shear loads, siderail bending moments, and siderail deflection. A mathematical model was developed based on elastic properties of the structural members of the tractor frame and fifthwheel assembly. The study includes a comprehensive design evaluation as a function of the following parameters: attachment bolt loads, tractor frame characteristics, fifthwheel frame attachment support rigidity, and effect of applying kingpin load through the siderail shear center. As a conclusion of this study, it was found that a six-bolt frame mount support consisting of two three-bolt patterns located at the mount extremes produces the lowest lead bolt load because the bolts are concentrated in a localized region, thus, the other bolts inherit a portion of the load. Moreover, tractor frame performance with on-highway kingpin

loads, 26,000 lbs. vertical plus 20,000 lbs. fore, is basically unchanged regardless of the type of fifthwheel mount design analyzed.

Dixon [8] accomplished a research study to establish practical fundamentals affecting fifthwheel coupler to frame attachment performance in commercial on-highway vehicle service. The analysis was presented through comparative studies of several fifthwheel attachment proposals under measured impact and dynamic load conditions. A mathematical program of analysis techniques was developed for showing correlation between service life and design variables. This program includes accurate measurements from the field environment, power spectra density analyses, and cumulative damage analyses. The results indicate that the life characteristic varies with the number of bolts in the pattern and inversely with bolt span width. Finally, Dixon emphasized that proposed systems must experience controlled tests for severe duty customer service even though a standardized coupler attachment meets the overall requirements for line haul operation.

Škorjanc et al. [9] used a Computer-Aided Design (CAD) tool for geometry modeling and finite element analysis (FEA) to accurately predict stresses on the bearing, holder, and top plate of a fifthwheel. The purpose of this study was to design a lighter fifthwheel than the current model (Fifthwheel Model SP201) and to successfully reduce weight by 18 kg without sacrificing the original functionality. This reduced weight can contribute to lower manufacturing costs and fuel efficiency during tractor operation.

In 2002, Ibrahim [10] proposed a three dimensional mathematical modeling technique to investigate the random vibration response of a 3-axle tractor-semitrailer system considering fifthwheel types and their associated kinematic constraints. The vehicle was excited by the road surface irregularities with different roughness levels. In this study, Ibrahim found that the conventional semi-oscillating fifthwheels increased the coupling between the tractor and semitrailer and accelerated their roll responses. However, the proposed fully oscillating fifthwheels offered significant improvements in the roll

responses of both tractor and semitrailer due to the compensation of its torsional spring and damper that reduces the torque and twist transfer. In addition, tractor roll response was improved by increasing the torsional flexibility of the tractor frame.

DeRegnaucourt [11] conducted experimental tests on tractor-semitrailer coupling. DeRegnaucourt measured a longitudinal peak kingpin force of 155,910 N (35,050 lb) and a tractor deceleration of $2.2g's^{(2)}$ at a coupling impact speed of 3.0 km/hr (1.89 mph) with a tractor whose weight was 72,950 N (16,400 lb). Based on this measurement, Janeway [12] determined a resultant deflection rate of the tractor structure in order to calculate a maximum coupling speed of 5.2 km/hr (3.23 mph) that would not exceed the approved load limit on the kingpin during that time, 266,890 N (60,000 lb). In this calculation, the semitrailer is in solid contact with an unyielding loading dock, and driving power and braking were not considered.

The equation that Janeway used for this calculation was developed mainly based on vehicle design parameters of a tractor-semitrailer and the principle of energy conservation. In other words, the kinetic energy of a tractor, one half of tractor mass times its velocity square ($\frac{1}{2} * m * v^2$), should be equal to the total work done on all components of the tractor-semitrailer system during coupling. For example, during coupling, the tractor's pitching motion due to suspension spring compression at the rear axle and extension at the front axle, tire deflections, and the elastic bending of the tractor frame absorb a large amount of the kinetic energy of the tractor.

Similarly, Janeway stated that the outstanding sources of coupling impact energy absorption in the tractor-semitrailer system are due to elastic structural deflections of tractor and semitrailer chassis. The tractor shows nearly twice as much energy absorbing ability as the semitrailer. In a typical case, 86% of the total energy is absorbed by the tractor and semitrailer chassis structural components. The rest of the total energy (14%)

² $1g = 9.81 \text{ m/s}^2$.

is absorbed by the tractor's suspension; this is the result of a long wheelbase and stiff suspension springs. Any appreciable increase in rigidity of trailer and/or tractor structures will require additional compensating measures to provide adequate energy absorption capacity.

1.3.3 Comparison of Maximum Kingpin Load Definitions

Sweatman [6] introduced the maximum allowable longitudinal fifthwheel force (E_o) calculated in Equation 1.7. The D-value is outlined in SAE Standard J133 and is calculated in Equation 1.1.

This section compares and discusses the E_o and D-values between Sweatman's 6-axle tractor-semitrailer and the tractor-semitrailer selected for this thesis. Sweatman's 6-axle tractor-semitrailer has a GVW of 410,524 N (92,290 lb) and the selected tractor-semitrailer has a GVW of 406,253 N (91,330 lb). Weight data is summarized in Figure 1.9 and the comparison of the E_o and D-values is shown in Table 1.1. The values for Sweatman's 6-axle tractor-semitrailer shown in Table 1.1 are given in the reference [6].

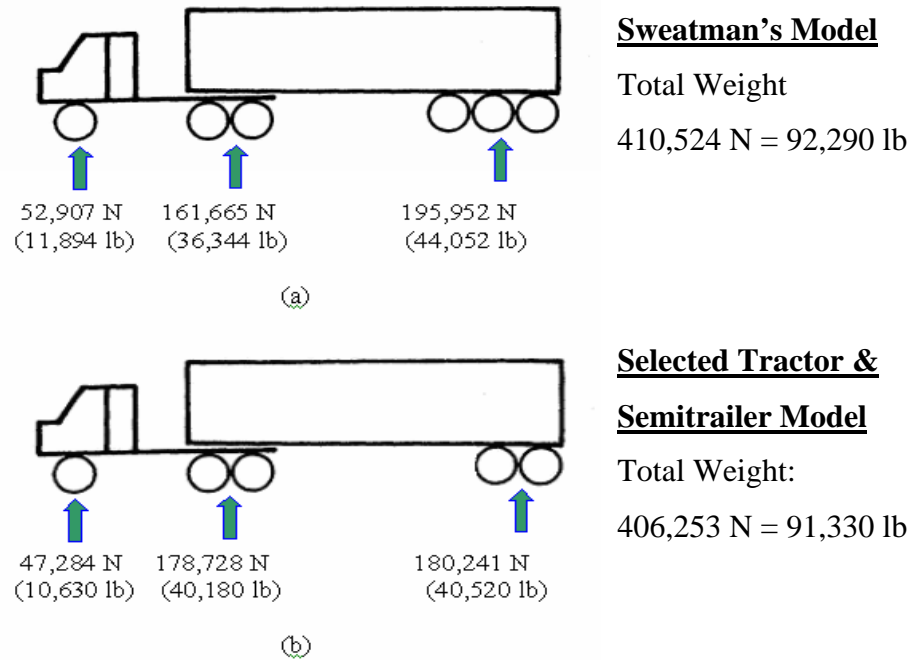


Figure 1.9: (a) 6-axle tractor-semitrailer [6] and (b) tractor-semitrailer selected for this report

Table 1.1: Comparison between the two tractors and semitrailers

	Gross Vehicle Weight (M_1)	Total Tractor Weight (M_0)	Vertical Load on Drive Axle (d)	Calculated Maximum Allowable Longitudinal Force on Kingpin (E_o)	Calculated D-value
6-Axle Tractor-Semitrailer	410,524 N (92,290 lb)	93,079 N (20,925 lb)	161,665 N (36,344 lb)	100,329 N (22,555 lb)	99.7 kN
Selected Tractor-Semitrailer	406,253 N (91,330 lb)	73,884 N (16,610 lb)	178,728 N (40,180 lb)	100,802 N (22,661 lb)	111.2 kN

It should be noted that Sweatman's tractor-semitrailer is heavier by 4,271 N (960.2 lbs.) than the selected vehicle. Both the D-value (Equation 1.1) and E_o (Equation 1.7) of the selected tractor-semitrailer are higher than those of Sweatman's tractor-semitrailer. This

is because the vertical load on the drive axles of the selected tractor-semitrailer is higher than Sweatman's tractor-semitrailer. This means that the sample tractor-semitrailer selected for this research needs a stronger kingpin and fifthwheel even though its GVW is lighter. Therefore, it is more important to lower the tractor's drive axle loads than to lower the GVW to relieve the kingpin and fifthwheel forces.

So far, D-values and maximum longitudinal kingpin forces have been investigated only with respect to the different axle load distributions. However, other vehicle design parameters such as suspension, truck dimensions, and wheelbase should be also taken into consideration to thoroughly investigate the kingpin forces during different operating maneuvers of the tractor-semitrailer.

1.3.4 Coupling and Docking Simulations Using DADS

Previous coupling simulations were performed by the Vehicle Dynamics and Simulations Research Center (VDSRC) using DADS[®] rigid body simulation software [1]. CADSI-DADS[®] is a computer aided engineering software developed by LMS-CADSI Inc. It is widely used to predict the behavior of single or multi-body mechanical systems. The model included a tractor, a semitrailer, five axles, suspensions, a fifthwheel, and a kingpin. The model was designed to simulate pitch and roll motion between the tractor and semitrailer. Also, five auxiliary bodies were included between axles and chassis to provide axle roll, vertical relative motion, and auxiliary roll stiffness. Figure 1.10 shows the completed tractor-semitrailer model.

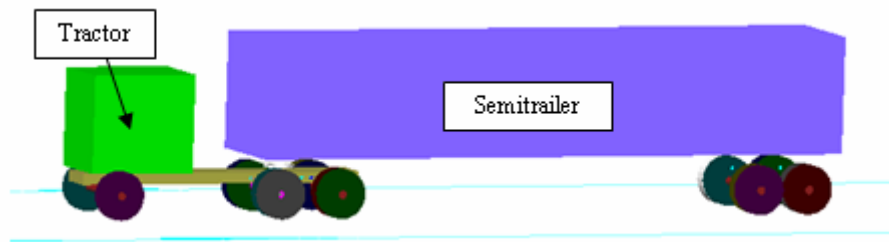


Figure 1.10: Five-axle tractor-semitrailer DADS[®] model [1]

1.3.4.1 DADS[®] Coupling Simulation

The coupling operation of the tractor with semitrailer was simulated in order to predict a longitudinal kingpin force. In order to investigate longitudinal kingpin forces at various coupling speeds, the tractor and semitrailer models were initially separated as shown in Figure 1.11. Then, the tractor was given various initial backward velocities towards the semitrailer. No drive torque is considered to move the tractor. Impact speeds from 1.6 to 6.4 km/h (1.0 to 4.0 mph) were investigated. The semitrailer was stationary on the ground and was constrained to prevent rearward motion during coupling.

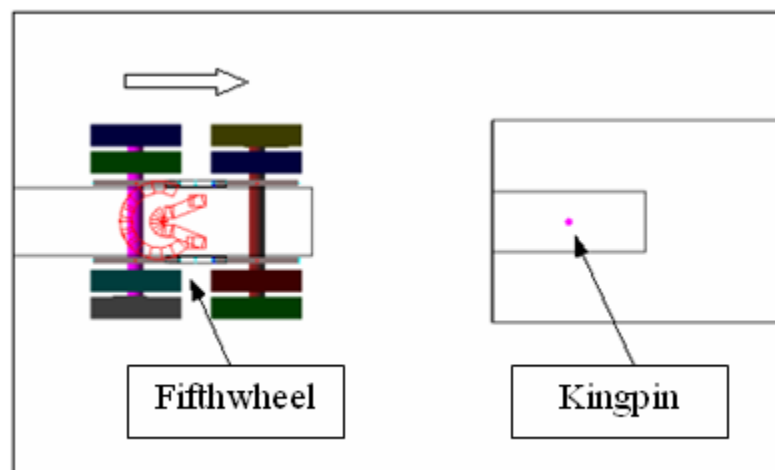


Figure 1.11: Coupling Model

When the moving fifthwheel hit and locked with the kingpin, the tractor decelerated very quickly to a stationary state. High inertial forces exerted on the kingpin and fifthwheel were directly related to the speed of the tractor. In this study, maximum coupling speed was predicted without exceeding the maximum kingpin load specified in the SAE J133.

1.3.4.2 Validation of the DADS[®] Coupling Model

Before the coupling simulations were conducted, the tractor-semitrailer model needed to be validated by comparing an experimental measurement with its simulated result. For the validation of this model, the Static Fifthwheel Load (SFWL) of the selected vehicle model was reduced to 65,655 N (14,760 lb) to make the value comparable with the SFWL of DeRegnaucourt's test vehicle. Then, the coupling simulation was conducted at the same coupling speed of DeRegnaucourt's test, 3.0 km/h (1.89 mph), to compare the longitudinal kingpin load and tractor deceleration. Table 1.2 shows a comparison of this study's DADS[®] simulation results with DeRegnaucourt's measurement.

Table 1.2: Validation of DADS[®] Simulation Model [1]

	DeRegnaucourt's Tractor	Selected Tractor
Tractor total weight	72,950 N (16,400 lbs.)	73,395 N (16,500 lbs.)
Tractor sprung weight	47,574 N (10,695 lbs.)	47,627 N (10,707 lbs.)
Static fifthwheel load	65,655 N (14,760 lbs.)	65,655 N (14,760 lbs.)
Tractor Wheelbase (mm)	3,607 mm (142 in.)	4,623 mm (182 in.)
Longitudinal kingpin load	155,909 N (35,050 lbs.)	157,795 N (35,474 lbs.)
Tractor deceleration (g's)	2.20	2.23

As can be seen in Table 1.2, the two systems were very similar. The total weight of the selected tractor was slightly heavier than that of DeRegnaucourt's tractor by 445 N (100 lb)—a 0.14 % difference. Each tractor's sprung weight was even closer with only a 0.11% difference. Therefore, as expected, the selected vehicle's longitudinal kingpin

load and tractor deceleration were slightly higher than those measured for the DeRegnaucourt's truck. The longitudinal kingpin load of 157,795 N (35,474 lbs) for the selected tractor-semitrailer was comparable to the lower longitudinal kingpin load of 155,909 N (35,050 lbs.) measured by DeRegnaucourt. The tractor decelerations were also quite similar. The selected tractor deceleration was found to be 2.23 g's, which is just 1.4% greater than that measured on DeRegnaucourt's tractor (2.20 g's). These results were considered be reasonable, thus successfully validating the model.

1.3.4.3 DADS[®] Coupling Simulation Results

After successful validation of the model, coupling simulations with different coupling speeds were conducted. The predicted tractor peak deceleration and longitudinal kingpin loads are plotted in Figure 1.12 and Figure 1.13, respectively.

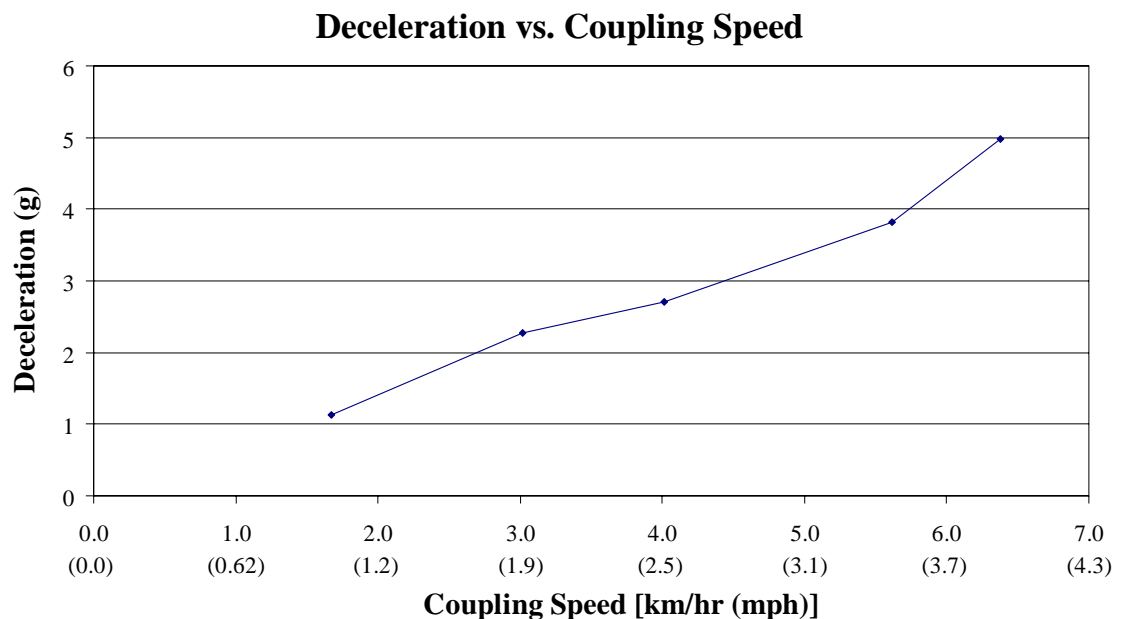


Figure 1.12: Tractor Deceleration vs. Coupling Impact Speed [1]

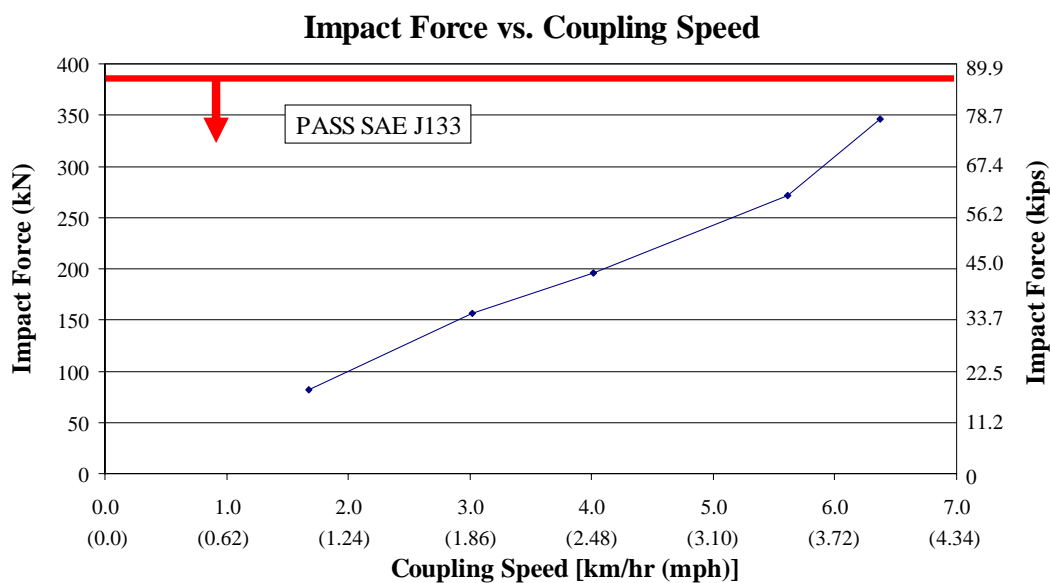


Figure 1.13: Kingpin Force vs. Coupling Impact Speed [1]

As can be seen from the deceleration and impact force plots, both deceleration and impact force are directly related to coupling speed. The kingpin of the selected tractor-semitrailer is required to withstand a horizontal single load up to 381,664 N (85,802 lb) according to the SAE J133. As can be observed in Figure 1.13, coupling impact speeds up to 6.4 km/hr (4.0 mph) do not exceed the single load limit defined by SAE Standard J133. ISO Standard 8717 defines a maximum horizontal test load equal to $0.6 \times D$ -Value (Equation 1.6). For the kingpin in operation with a D-Value of 210 kN (47,210 lb), the maximum longitudinal load calculated is 126 kN (28,326 lbs.). Interpolation of this value on the graph in Figure 1.13 corresponds to a maximum coupling speed of 2.48 km/hr (1.54 mph).

1.3.4.4 Investigation of the effect of SFWL

A short investigation into the effect of SFWL was undertaken using the validated DADS[®] coupling model. The semitrailer weight was increased to achieve a SFWL of 152,618 N

(34,310 lb), and the coupling simulation was ran with an impact speed of 3.0 km/h (1.89 mph). The kingpin force and tractor deceleration for the two SFWL values are shown in Table 1.3.

Table 1.3: Comparison between different SFWL values at the impact speed of 3.0 km/hr (1.89 mph)

SFWL	65,655 N (14,760 lbs)	152,618 N (34,310 lbs)
Longitudinal Kingpin load	157,795 N (35,474 lbs)	173,431 N (38,989 lbs)
Tractor Deceleration	2.23 g	2.49 g

It was found that the SFWL indeed affected the longitudinal kingpin force and tractor deceleration. This was thought to be due to a pitching motion of the semitrailer. This study concluded that it is important to reduce the SFWL in order to reduce the impact force on the kingpin during coupling operations. Although modern manufacturing processes can provide very strong kingpins to prevent failure of the kingpin itself, it is possible for the kingpin support structure to fail. The weld or bolt junction that connects the kingpin to its supporting structure on the semitrailer should be manufactured to endure those impact forces generated during coupling. This study recommended a standard procedure be developed for kingpin installation.

1.3.4.5 DADS[®] Docking Simulation and Results

A docking model of the tractor-semitrailer was developed to simulate docking operations at various speeds from 1.6 to 7.4 km/h (1.0 to 4.6 mph). These simulations were used to predict the longitudinal kingpin loads. No driving and braking efforts were considered during the docking maneuver and cushioning rubber material was attached on the top of the loading dock. The tractor was given an initial velocity to move the tractor-semitrailer

towards the loading dock until the rear of the semitrailer impacted the cushioning material on the dock. Figure 1.14 shows the docking model.

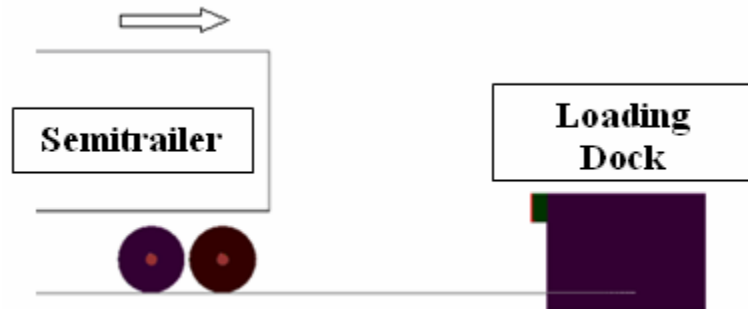


Figure 1.14: DADS Docking Simulation Model [1]

During docking, rubber material deformation on the dock was observed. The rubber deformation dissipates impact energy. Figure 1.15 shows the tractor deceleration versus docking speed graph. The longitudinal kingpin force versus docking speed graph is shown in Figure 1.16.

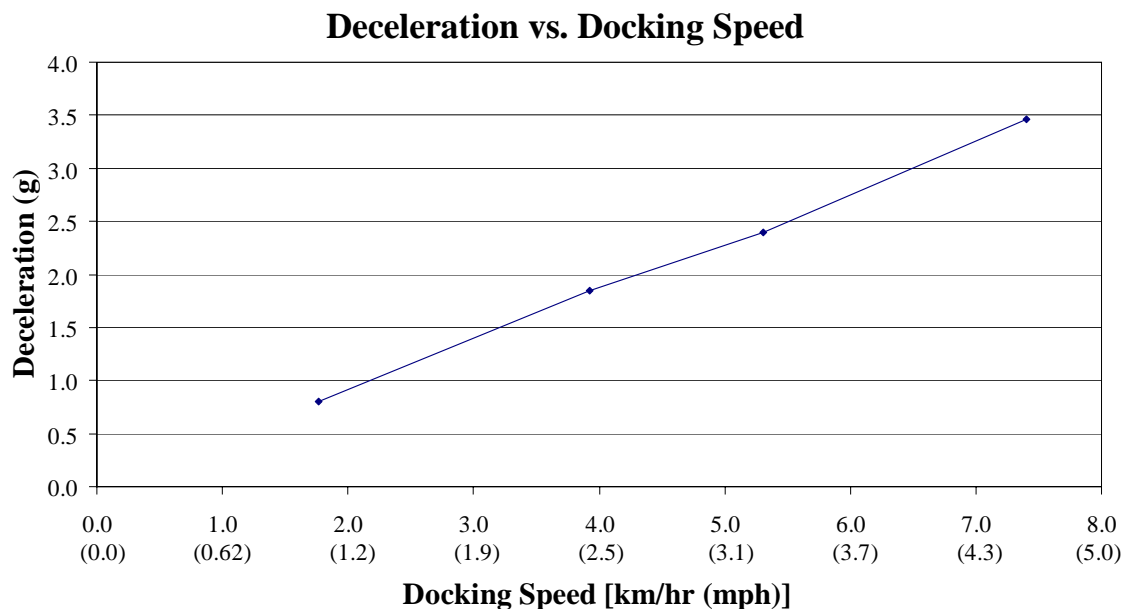


Figure 1.15: Tractor Deceleration vs. Docking Speed [1]

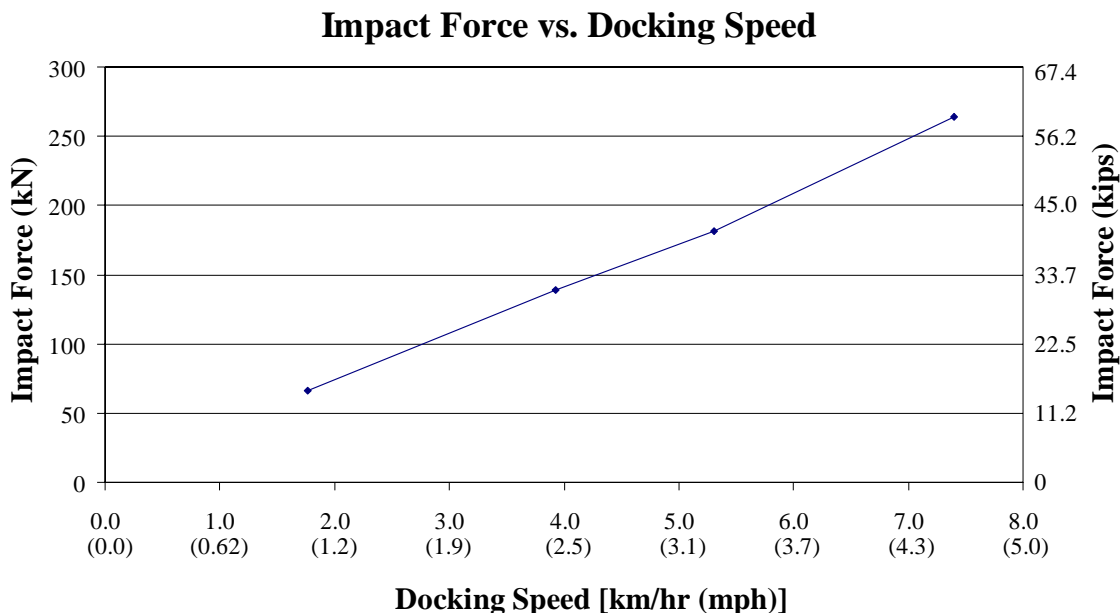


Figure 1.16: Longitudinal Kingpin Force vs. Docking Speed [1]

In both deceleration and impact force plots, the simulated values increase linearly. The kingpin forces from the docking simulations were found to be lower than those forces in the coupling simulations at the same speeds. For example, at the speed of 3.2 km/h (2.0 mph), the docking simulation yielded a tractor deceleration of 1.5 g and longitudinal kingpin force of 111,210 N (25,000 lb), whereas the coupling simulation at the same speed showed a tractor deceleration of 2.6 g and a longitudinal kingpin force of 177,928 N (40,000 lb).

Generally speaking, the longitudinal kingpin force during docking simulations corresponded to about 60% of the longitudinal kingpin force during coupling simulations at the same speed. During the docking operation, more parts of the vehicle such as semitrailer suspension, tire deformation, and the rubber material on the loading dock are involved in dissipating the docking impact energy. This is why lower impact forces were observed on the kingpin during docking compared to the forces observed during coupling at the same speed. The predicted impact forces on the kingpin during docking operations

passed the SAE Standard J133 test load requirement. However, if the loading dock does not feature rubber energy dissipation devices and a solid concrete dock is impacted, this conclusion may change.

1.4 Thesis Objectives

The objective of this thesis is to investigate the reaction forces seen at the kingpin during a coupling maneuver between a tractor and semitrailer using Finite Element Analysis. This requires finite element models of tractor-semitrailer systems to be created, developed, and validated. Another purpose of this work is to analyze the effect of various forces on the kingpin supporting structure of a semitrailer.

Also, a translational damping device is simulated to mitigate the kingpin impact force during coupling. The purpose of these simulations is to investigate the effectiveness of such a system and to obtain an optimized set of damping device parameters for a specific tractor-semitrailer system.

1.5 Thesis Outline

Chapter two presents the two main finite element models and gives an overview of the modeling approach. Chapter three discusses the coupling tests and tractor-semitrailer model validation. Chapter four discusses the tests completed at Mack Trucks' facility and the model validation completed with their results; chapter four also includes an analysis of a fifthwheel damping system incorporated into the Mack Trucks finite element model. Chapter five presents the results from an elastic kingpin supporting structure model. Chapter six discusses the conclusions of this thesis and presents suggestions for future work.

Chapter 2

DEVELOPMENT OF TRACTOR-SEMITRAILER FEA MODEL

This section describes the development of the FEA tractor-semitrailer models that were used to perform the coupling simulations. The objective is to design a finite element model capable of being versatile and easily manipulated to provide various predictions of displacements, velocities, and accelerations of both the tractor and semitrailer.

In the past, Škorjanc et al. [9] used a Computer Aided Design program for geometric modeling and an FEA program to accurately predict stresses on the bearing, holder, and top plate of a fifthwheel. The purpose of this study is to design a lighter fifthwheel than the current model, SP201 fifthwheel. The author successfully reduced the weight by 18 kg (39.7 lbs) without sacrificing the original functionality. This reduced weight can improve the manufacturing cost economy and the fuel efficiency during tractor operations.

The finite element models of the tractor-semitrailer systems used for the research in this thesis were built using PATRAN[®] and PAM System. PATRAN[®] is a preprocessing and Computer Aided Engineering (CAE) software program developed by MSC systems, and PAM System is a model developing and solving software program developed by the ESI Group. PAM System includes very advanced modeling and surfacing tools which make it possible to create the finite element models necessary for analysis and validation.

2.1 FEA Models of Fifthwheel and Kingpin

The initial Finite Element modeling began with a model of a fifthwheel and a kingpin. These are the two most important parts of the model. The modeled kingpin is a two-inch mushroom type constructed of solid elements using PATRAN[®], then imported into PAM,

and welded to the semitrailer bolster plate. Figure 2.1 shows the finite element kingpin and a photo of an actual kingpin.

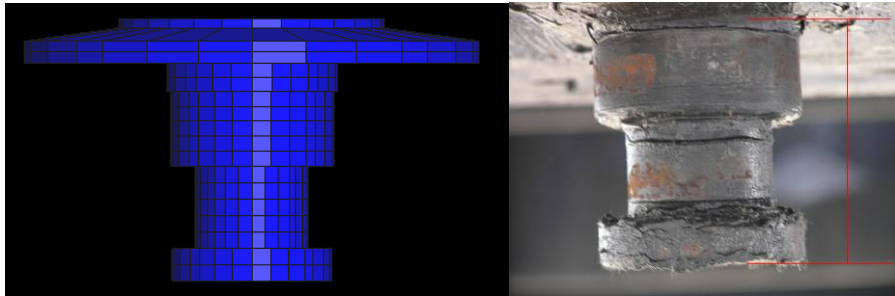


Figure 2.1: Kingpin finite element model and photo

The fifthwheel model was constructed of shell elements and is free to rotate around the traverse axis that represents the fifthwheel load pin constraint. This load pin is supported by two brackets which are welded to the tractor chassis. Figure 2.2 shows the finite element model of the fifthwheel along with a photo of an actual fifthwheel.

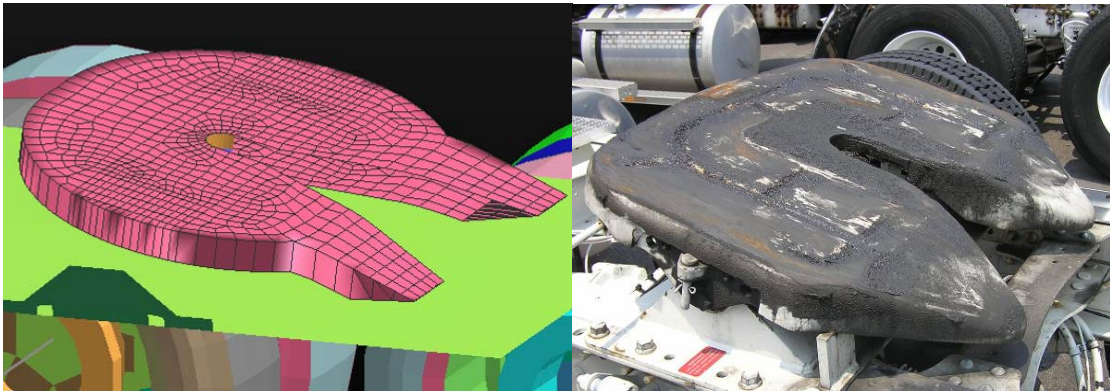


Figure 2.2: Fifthwheel finite element model and photo

Figure 2.3 shows a wire frame close up view of the bolster plate with the attached kingpin in a coupled position with the fifthwheel. To reduce simulation time the fifthwheel and semitrailer plates are represented by the outer contact surfaces.

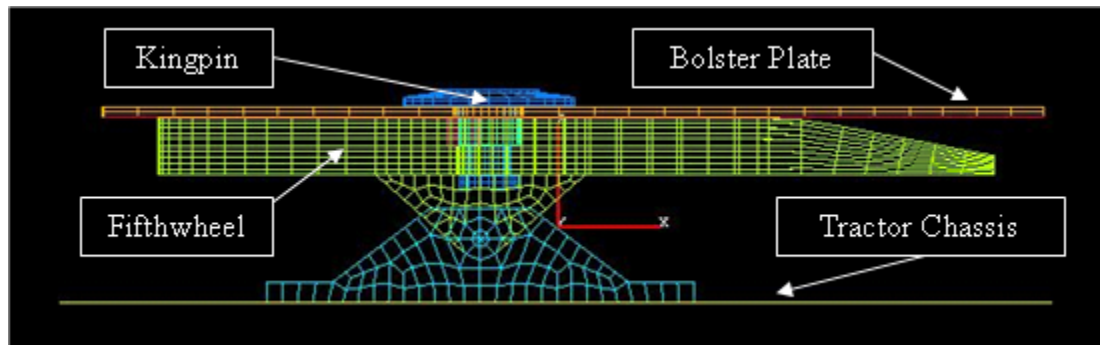


Figure 2.3: FEA model of the coupled fifthwheel and kingpin

2.2 ARL Tractor & Single-Axle Semitrailer Model

The first validation tests were conducted using a tractor-semitrailer owned by ARL. A tractor-flatbed semitrailer model was constructed to simulate the ARL coupling tests. The model consists of a tandem-axle tractor and a single-axle flatbed trailer. The weight data of the tractor and semitrailer model are shown in Table 2.1.

Table 2.1: Weight data of ARL tractor-semitrailer used to conduct coupling tests

	Weight
Tractor	72,239 N (16,240 lb)
Semitrailer	38,344 N (8,620 lb)

Figure 2.4 shows the FEA model of the three-axle tractor and single-axle flatbed trailer.



Figure 2.4: ARL tractor-flatbed semitrailer FEA model

Figure 2.5 and 2.6 show top views of this tractor and semitrailer FEA models, respectively.

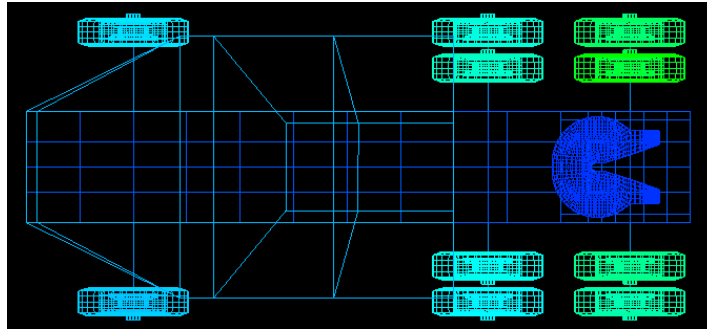


Figure 2.5: Top view of ARL tractor model

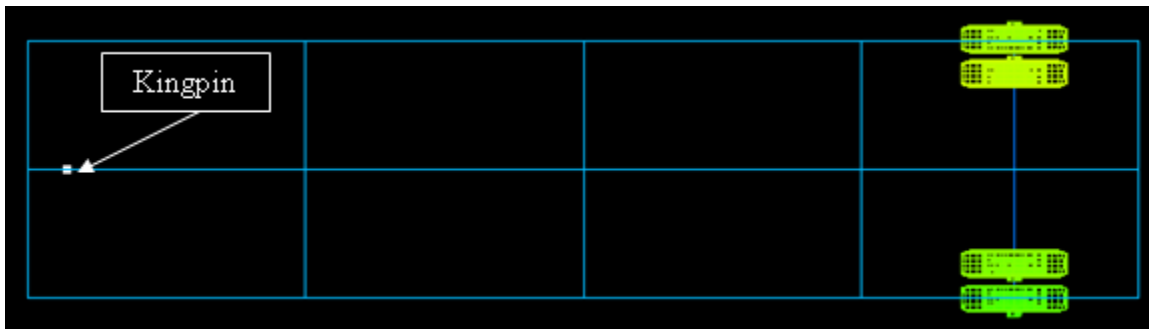


Figure 2.6: Top view of ARL semitrailer model

The suspensions of the tractor and semitrailer are equipped with typical leaf springs and shock absorbers. The tires are inflated to 110 psi and the tire/road coefficient of friction can be varied to represent the desired road surface.

Revolute joints were constructed between the axles and wheels, which enables wheel rotation. The stationary semitrailer was supported by two supports in the front and by the wheels and suspensions in the rear. During coupling simulations, the wheels of the trailer are free to slide in the longitudinal direction but are not allowed to rotate (braked). An initial velocity is applied to the tractor's center of gravity and the tractor rolls freely until the kingpin is coupled with the fifthwheel, as shown in Figure 2.7.

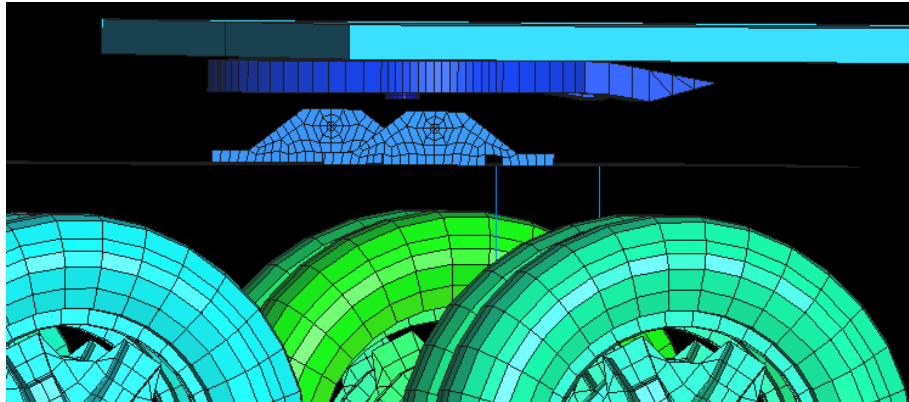


Figure 2.7: Coupled ARL tractor and semitrailer

2.3 Mack Trucks Tractor & Dual-Axle Semitrailer Model

Mack Trucks in Allentown, Pennsylvania permitted ARL to conduct coupling tests using Mack test tractors and trailers. A Fontaine brand trailer was selected for use in the coupling tests. The weight on this trailer could easily be added or removed to vary the weight distribution during testing. The dimensions of the Mack truck and Fontaine semitrailer were obtained to complete construction of the virtual test tractor-semitrailer model using MSC.PATRAN[®]. Dimensions for the truck and trailer are shown in Figures 2.8 and 2.9, respectively.

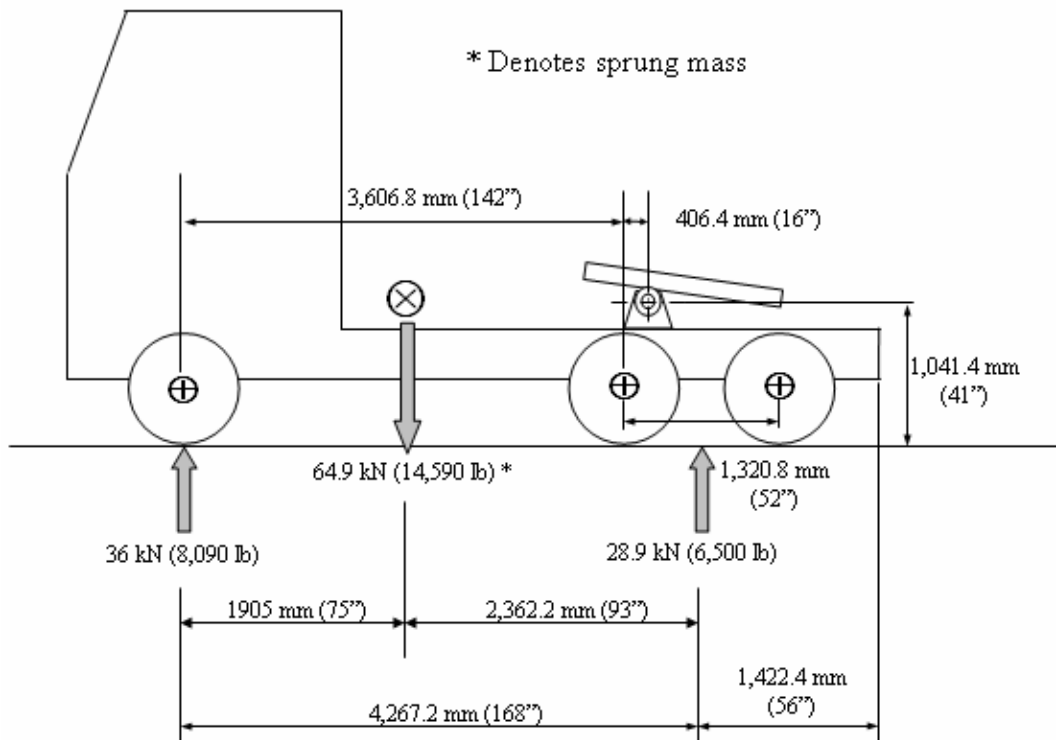


Figure 2.8: Mack Trucks' truck dimensions

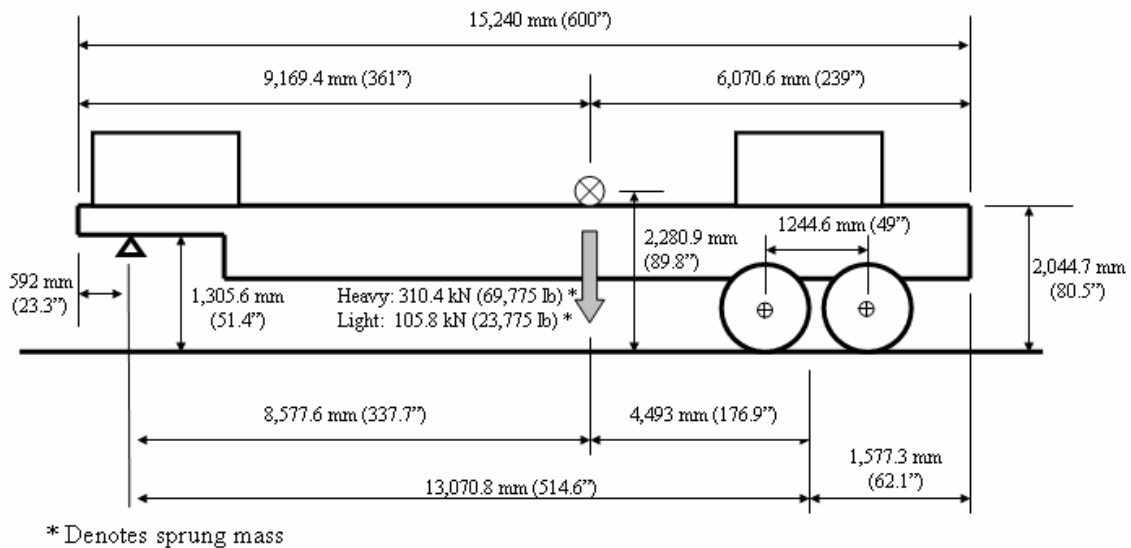


Figure 2.9: Mack Trucks' Fontaine trailer dimensions

With the measurements known, an accurate and efficient finite element model of the test trailer was created. The construction of the full test trailer model began by designing the kingpin and its surrounding support structure. All components of the kingpin support structure were modeled using solid elements. Solid elements were used to represent the kingpin support structure because during the coupling simulations it is necessary to analyze the stresses and forces transmitted from the coupling impact. Figure 2.10 juxtaposes the virtual model of the kingpin support structure with an actual picture taken from the Fontaine test trailer. The support structure was later modified to contain only shell elements. This modeling change decreased the computation time drastically.

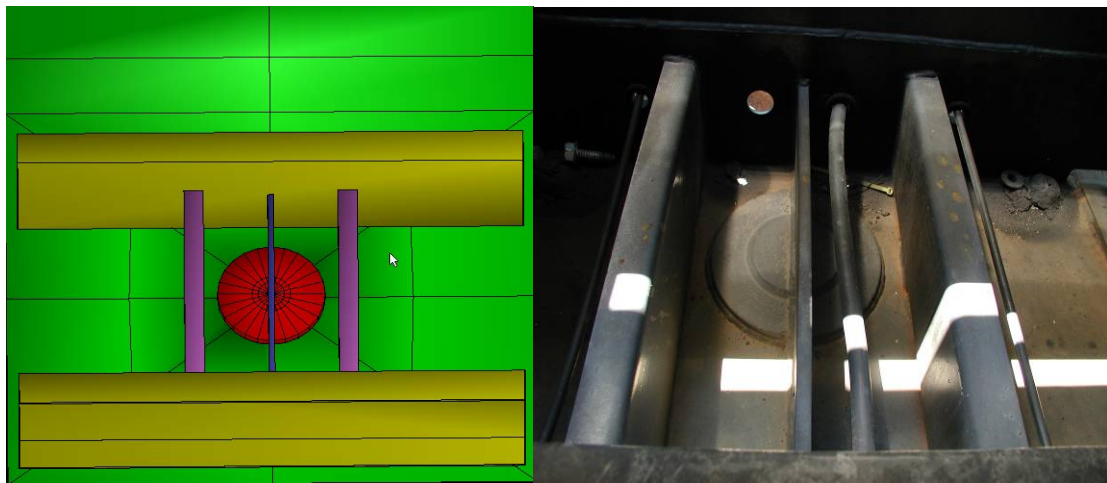


Figure 2.10: FEA kingpin support structure model and actual support structure

Two box masses were added to the trailer allowing easy manipulation of the total weight and weight distribution of the trailer. The Mack Trucks' test semitrailer and kingpin support structure models were imported and then merged with a truck model using PAM Visual-Crash. Figure 2.11 shows the side view of the model, while Figure 2.12 shows the model during coupling alongside the actual tractor-semitrailer.

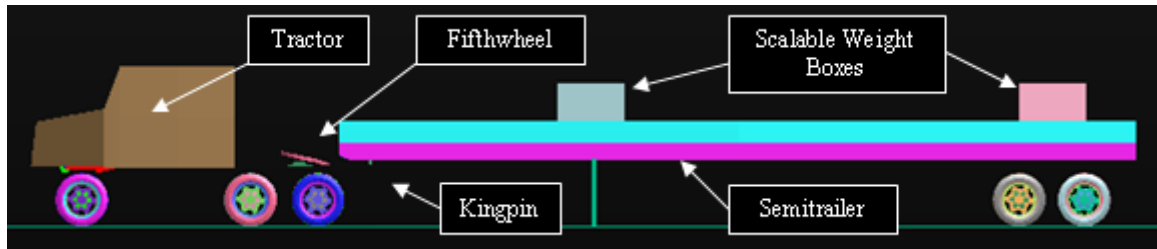


Figure 2.11: Mack Trucks' model side view

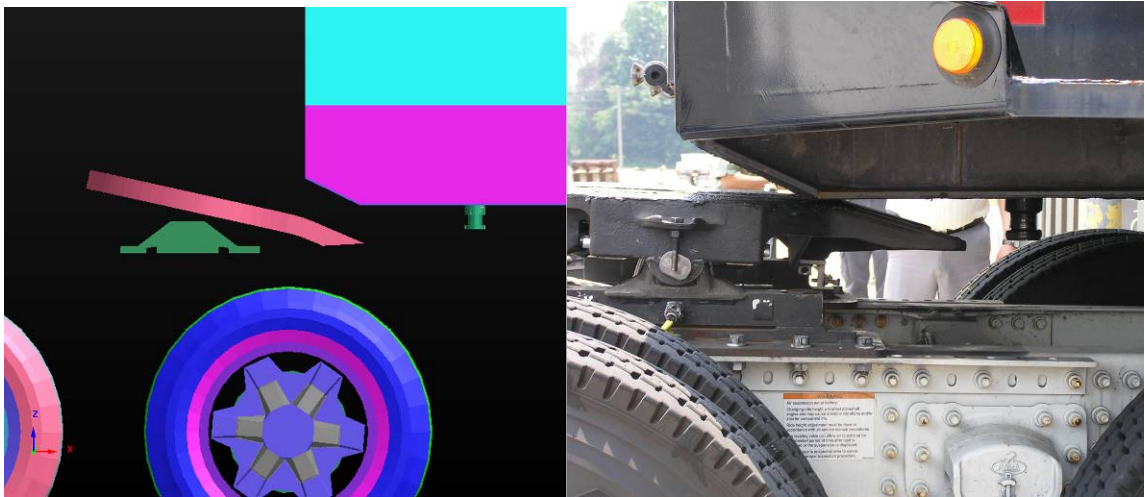


Figure 2.12: Actual and simulated fifthwheel and kingpin near coupling position

Figure 2.13 shows the truck, trailer, and kingpin support structure together in Visual-Crash. Figure 2.14 shows an isometric view of the entire model in PAM Visual-Crash environment.

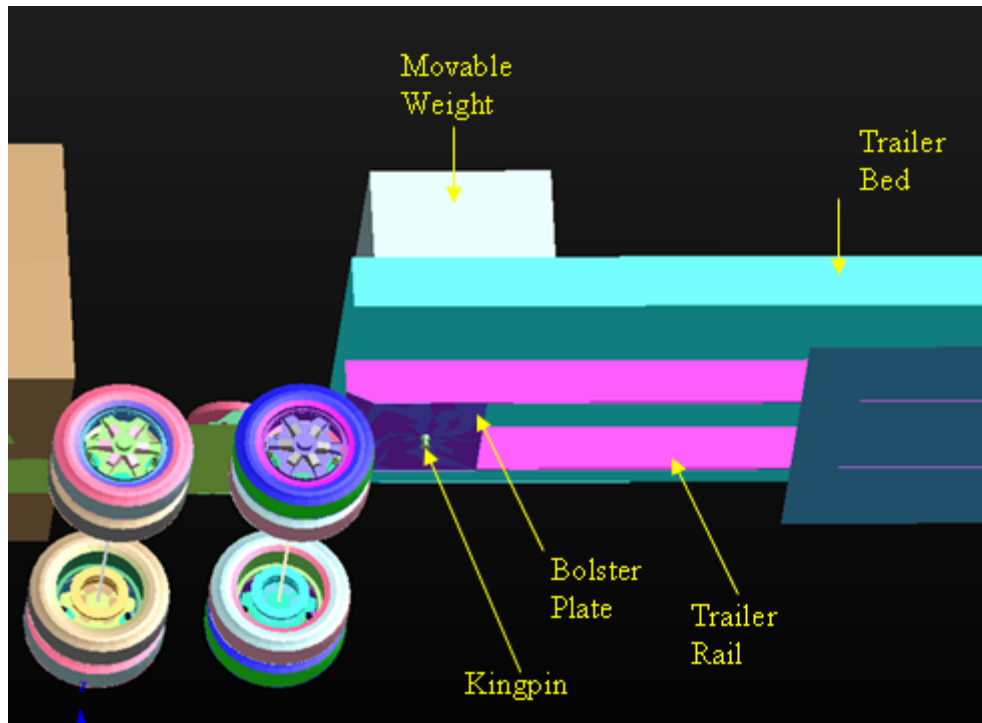


Figure 2.13: Bottom view of Mack Trucks' trailer model

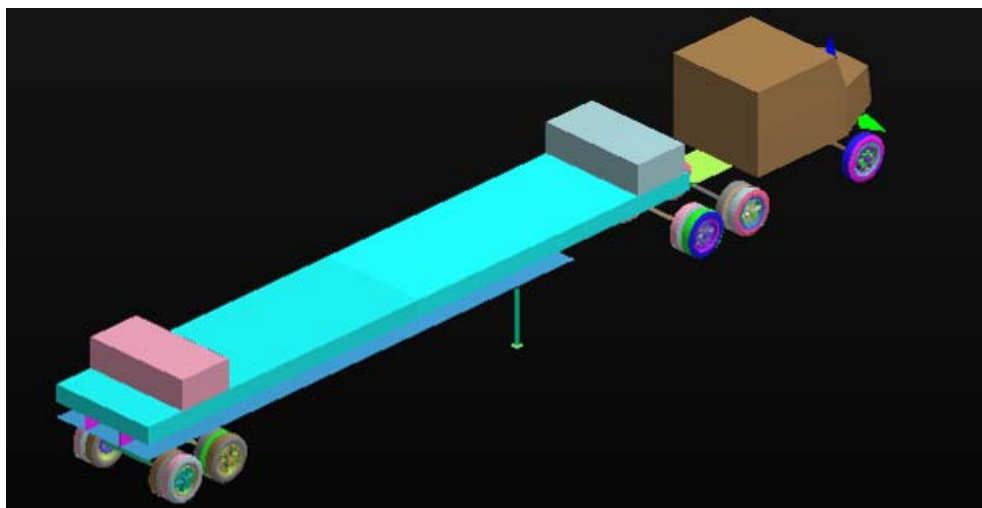


Figure 2.14: Full isometric view of Mack Trucks' simulated test tractor-semitrailer

The finite element model was generated to easily extract kingpin contact forces at various impact velocities. This model also included a longitudinal sliding fifthwheel mechanism for virtual testing of an energy dissipation system. The bracket displacements occurring during virtual tests using the longitudinal fifthwheel damping device can easily be plotted with respect to time. The spring stiffness and damping are easily adjusted for investigation into the design of such a damping system.

Chapter 3

ARL COUPLING TESTS AND MODEL VALIDATION

An ARL tractor chassis and semitrailer were instrumented with various accelerometers. The mass properties of the ARL coupling model are shown in Table 3.1.

Table 3.1: Weights of ARL tractor and single-axle semitrailer

	Weight
Tractor	72,239 N (16,240 lb)
Fifthwheel Vertical Load	16,503 N (3,710 lb)
Single-Axle Trailer	38,344 N (8,620 lb)

3.1 ARL Measurements

Both longitudinal and vertical sensors were placed on the truck and trailer, as shown in Figure 3.1.



Figure 3.1: Vertical and longitudinal accelerometers on the ARL tractor (left) and semitrailer (right)

A low speed tachometer system, shown in Figure 3.2, was assembled to measure the speed of the tractor. The tachometer data was processed and output to the digital readout display shown in Figure 3.3 for driver's use during actual testing. In addition, a Global Positioning System (GPS) was added to the tractor and to the flatbed trailer to provide additional velocity data for comparison purposes.

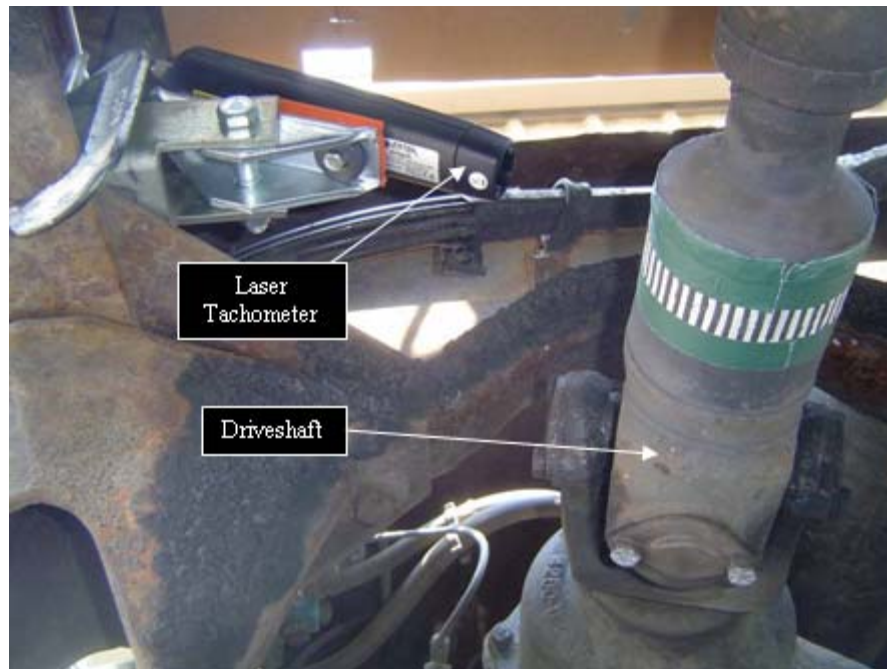


Figure 3.2: ARL low speed tachometer driveline measurement system



Figure 3.3: Digital display inside the tractor cab for low speed measurements

Data was collected at 102 kHz with two data acquisition systems, one each for the tractor and semitrailer. A wireless system was used for communication between the two data acquisition boxes for instantaneous viewing capabilities of each data channel.

3.2 ARL Model Validation

Three impact speeds were selected for simulation using the FEA model of the ARL tractor and single-axle semitrailer system. The longitudinal deceleration of the tractor was used for validation of the FEA simulation. Both the experimental and simulated decelerations were filtered at 60 Hz. The peak accelerations are shown in Figure 3.4. The average percent difference between the measured values and the FEA simulation is less than 33%, which is within accepted test tolerances.

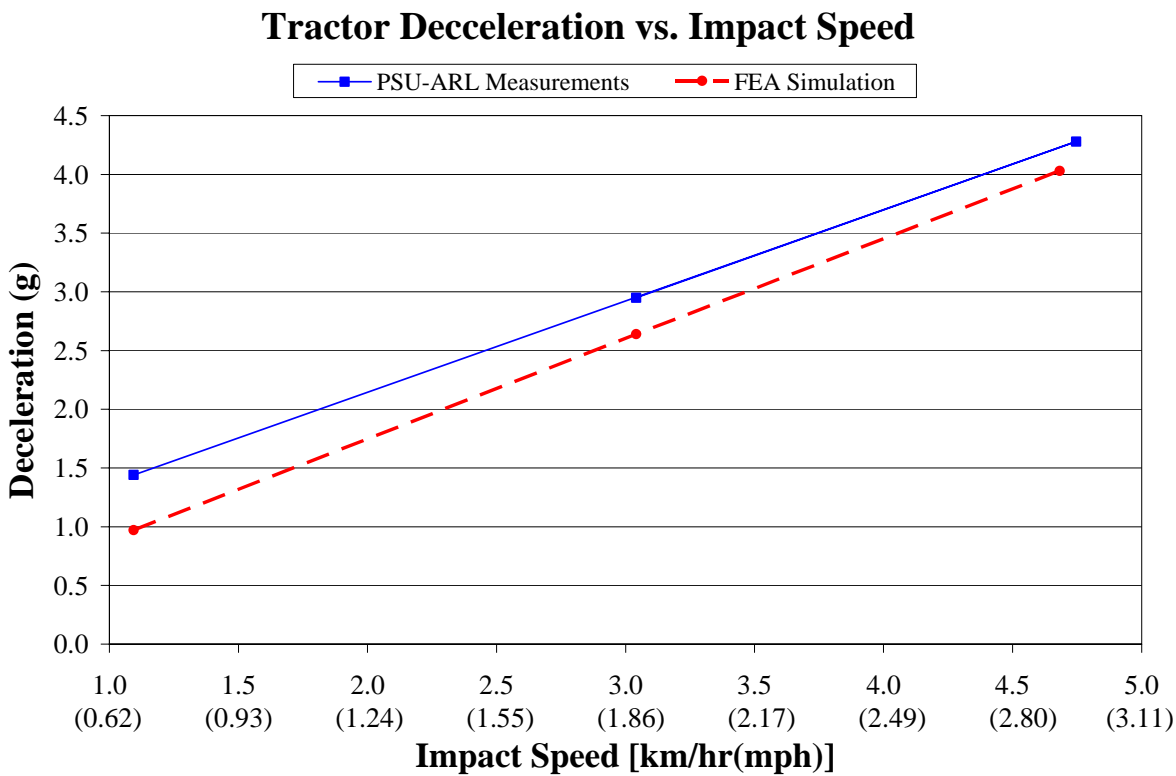


Figure 3.4: Validation comparison between ARL experimental measurements and FEA simulations

3.3 Preliminary Parametric Analysis of a Fifthwheel Damping System

Two sets of coupling simulations were conducted to investigate the effect of a fifthwheel damping device. The first set of simulations was conducted by restricting the fifthwheel to only rotate about a fixed bracket pivot joint. This “fixed bracket” coupling simulation was used as the baseline for mitigating loads transmitted to the kingpin in “sliding bracket” simulations. In the second set of coupling simulations, the fifthwheel was free to rotate about a bracket pivot joint which is allowed to translate in the longitudinal direction. A translational spring/damper joint was implemented in the longitudinal direction between the fifthwheel brackets and the tractor chassis. The translational spring and damper joint allows a percentage of the impact load to be transferred from kingpin to fifthwheel longitudinally.

The results of the fifthwheel damping system simulations are shown in Figures 3.5 to 3.7 at a coupling speed of 4.75 km/hr (2.95 mph). For the damping system under evaluation, three different spring stiffnesses were simulated using four different damping coefficients. These different variations of the translating fifthwheel were compared to the fixed fifthwheel system (with a bracket displacement of zero). The objective was to predict the optimal damping system that may be used for mitigation of the kingpin impact force specific to this vehicle configuration.

The damping system concept simulations showed lower kingpin impact force and tractor deceleration values with respect to the fixed bracket baseline values. An optimal damping system would reduce the tractor deceleration and impact force on the kingpin, while maintaining minimum bracket displacement. From the simulations performed, an optimum damping system could be selected. A suggested spring/damper system would include a spring with a 2.8 kN/mm spring constant and a 5 N-s/mm damper while only allowing 3.5 cm (1.38 in) of displacement.

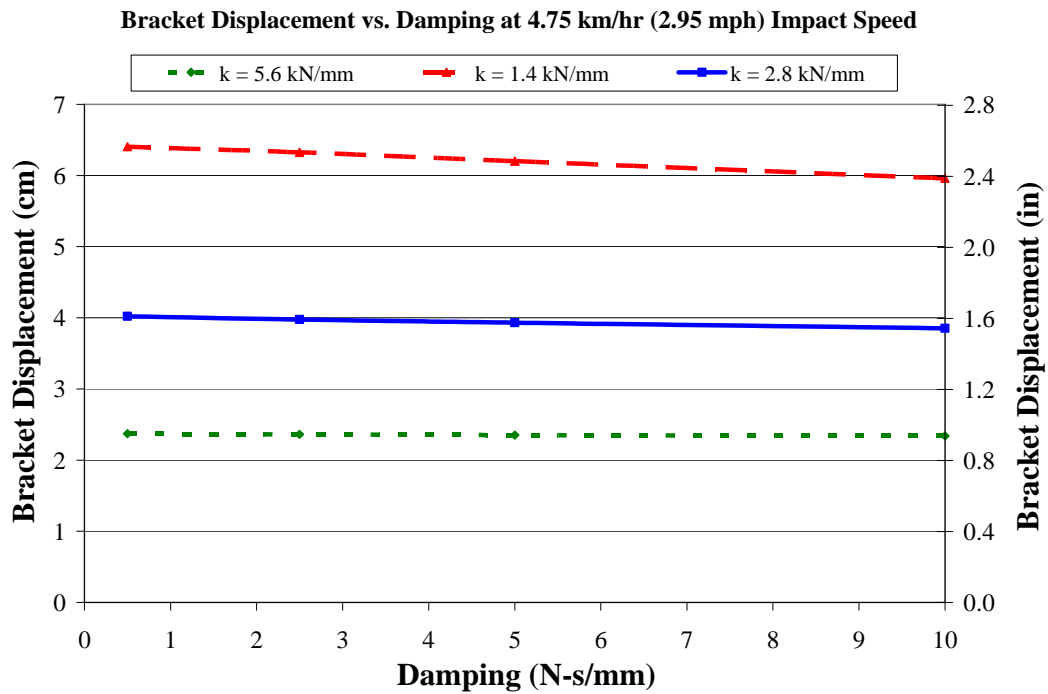


Figure 3.5: Bracket displacement of selected damping system parameters

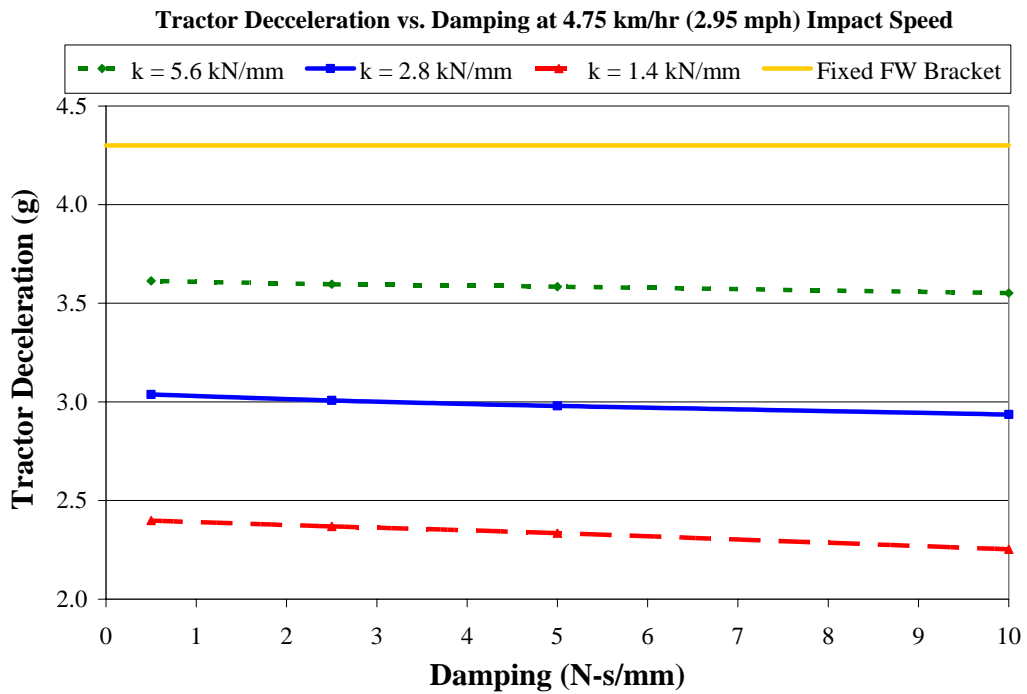


Figure 3.6: Tractor deceleration of selected damping system parameters

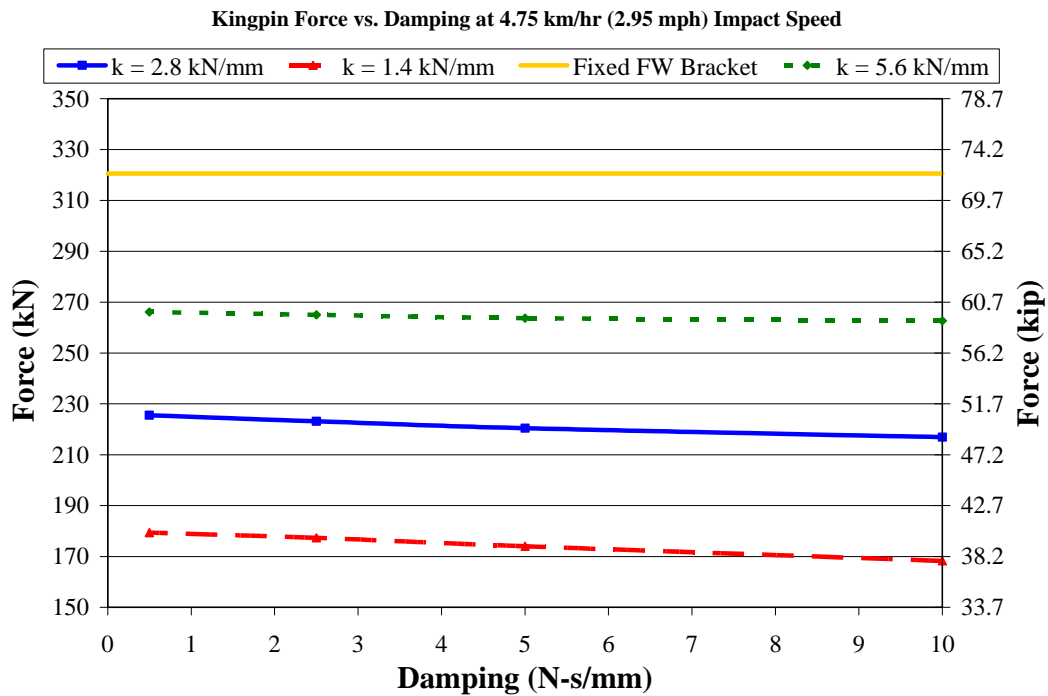


Figure 3.7: Kingpin impact force of selected damping system parameters

In order to determine the effect of semitrailer weight using the selected outputs of the damping system concept, a heavier trailer simulation was conducted. The trailer weight of 331,840 kN (74,600 kips) was chosen. The fifthwheel damping system was outfitted with a 2.8 kN/mm spring and a 5 N-s/mm damper. Table 3.2 shows the results from the semitrailer weight sensitivity analysis. The simulation indicates that a larger trailer weight has a direct effect on bracket displacement, tractor deceleration, and kingpin coupling force.

Table 3.2: Effect of semitrailer weight on coupling dynamics

Trailer Weight [kN (kips)]	Bracket Displacement [cm (in)]	Tractor Deceleration [g]	Coupling Force [kN (kips)]
38,344 (8,620)	3.86 (1.52)	2.93	221.2 (49.7)
331,837 (74,600)	4.50 (1.77)	3.40	252.0 (56.7)

Chapter 4

MACK TRUCKS COUPLING TESTS AND MODEL VALIDATION

Mack Trucks outfitted a tractor and semitrailer with accelerometers. A calibrated fifthwheel provided by SAF-Holland was used to obtain kingpin/fifthwheel impact forces. Deceleration and force data from Mack Trucks' tests will be compared to the data obtained from the virtual coupling of the trailer with a tractor. Table 4.1 shows the Mack Trucks' tractor weight and Fontaine semitrailer weights.

Table 4.1: Weights of Mack Trucks' tractor and Fontaine semitrailer

	Weight
Tractor	64.90 kN (14.590 kips)
Light Trailer	105.76 kN (23.775 kips)
Heavy Trailer	310.37 kN (69.775 kips)

4.1 Mack Trucks Measurements

The velocity of the tractor was captured to determine impact speed during tractor fifthwheel and semitrailer kingpin coupling. Deceleration of the tractor and acceleration of the semitrailer were measured at their respective centers of gravity with tri-axial accelerometers (Figure 4.1 and Figure 4.2). Also, fifthwheel forces were measured with the SAF-Holland fifthwheel, and the axle loads were measured.



Figure 4.1: Tractor accelerometer on Mack Trucks' instrumented tractor chassis

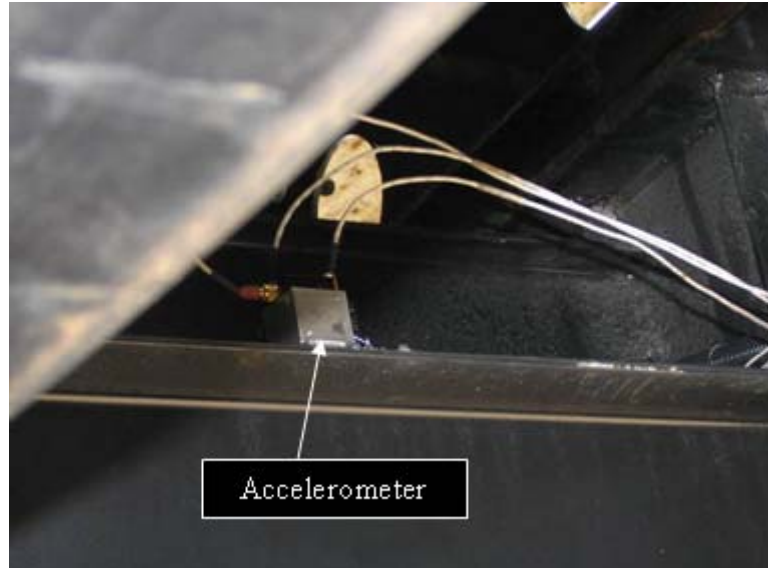


Figure 4.2: Trailer accelerometer on Mack Trucks' instrumented Fontaine trailer

4.2 Tractor Velocity Measurement Methods

Tractor impact speed was measured using two methods. The first used GPS provided by SAF-Holland and the second measured speeds using digital video. To determine the impact speed with digital video, the time that elapsed as the tractor axles passed between two painted lines was measured. This process is displayed in two frames visible in Figure 4.3.



Figure 4.3: Digital video frames used for impact speed estimation

Seven tractor-semitrailer couplings were performed with two different semitrailer loads—heavy (310.5 kN, 69.8 kips) and light (105.9 kN, 23.8 kips). The results of the experiment are compiled in Table 4.2.

Table 4.2: Mack Trucks' experimental measurements

Trailer Load	GPS [km/hr (mph)]	Video [km/hr (mph)]	Tractor Deceleration (g)	Coupling Impact Force [kN (kips)]
Heavy	2.24 (1.39)	2.25 (1.40)	2.48	180.59 (40.60)
Heavy	2.41 (1.50)	2.38 (1.48)	2.54	171.49 (38.55)
Heavy	2.77 (1.72)	2.46 (1.53)	3.00	202.53 (45.53)
Heavy	3.52 (2.19)	3.52 (2.19)	4.38	255.69 (57.48)
Light	2.41 (1.50)	1.85 (1.15)	1.75	137.05 (30.81)
Light	2.77 (1.72)	2.32 (1.44)	2.93	203.11 (45.66)
Light	3.70 (2.30)	3.23 (2.01)	3.44	259.79 (58.41)

As shown in Figure 4.4, the results obtained from GPS and digital video calculations correlated with the heavy semitrailer, however the light semitrailer did not match as well. It was found that the refresh rate on the GPS unit was low, and the speeds being measured at impact were not conducive to using the GPS technology for this measurement.

Tractor Deceleration Test Results Using Video and GPS Speed Measurement

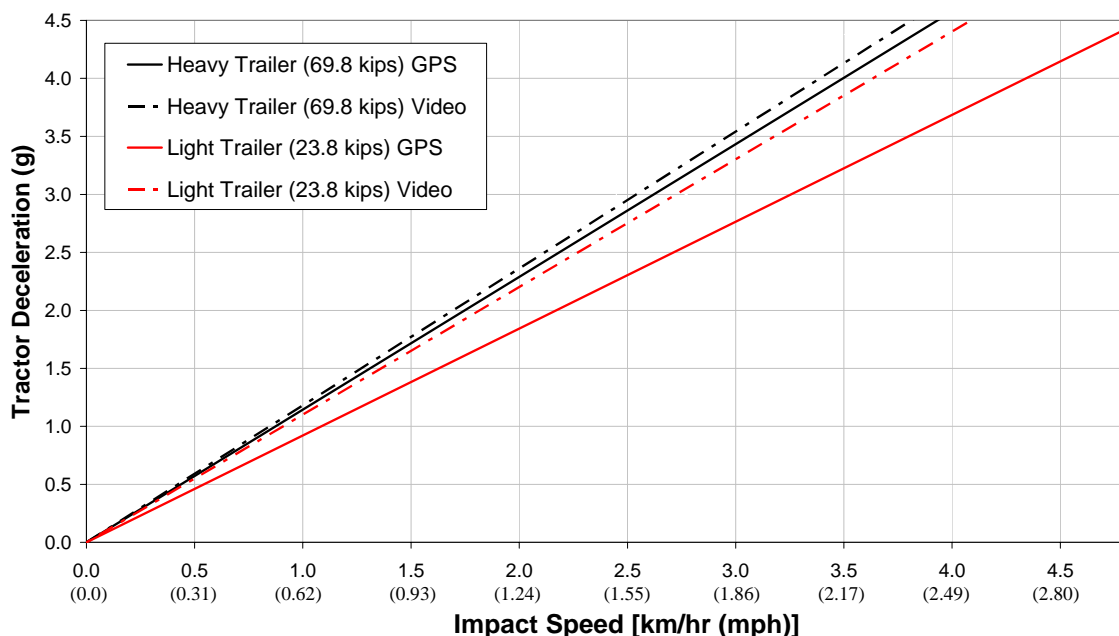


Figure 4.4: Tractor deceleration vs. impact speed (GPS and digital video) during Mack Trucks' coupling tests

During this phase of testing at Mack Trucks, an observation was made during the impact tests which resulted in some of the data being questionable. It was observed that the driver applied the brakes just before impact on some of the tests. This is apparent after inspecting the data presented in Figure 4.4. The lines representing the light trailer data show a significant difference in tractor deceleration between GPS and video speed measurement at the same impact velocity. In reviewing the heavy trailer data, the lines for the GPS and video measurements do not show a similar difference. Either the video data or the GPS data for the light trailer is in error. Knowing that the lightweight trailer data is in question requires that the tests be repeated at a future date and that the data not be used in this analysis.

In the process of recording the velocity using digital video, an accuracy concern was raised. The use of video to measure velocity is dependent on time measurement between

a set of marks. In order for the time measurement to be accurate and repeatable, a long distance is required between marks. After testing, the measured distance was not considered long enough for accurate impact speed measurements. Because of this concern, it was decided to use the GPS velocity data in all plots.

4.3 Mack Trucks Model Validation

Two sets of data were used to validate the FEA model. Decelerations at the center of gravity of the tractor and the measured kingpin impact forces were compared to the predicted data to provide model validation.

4.3.1 Tractor Impact Deceleration

Figure 4.5 shows the results for both experimental and simulated tractor decelerations at impact versus impact speed based on the GPS values from Table 4.2.

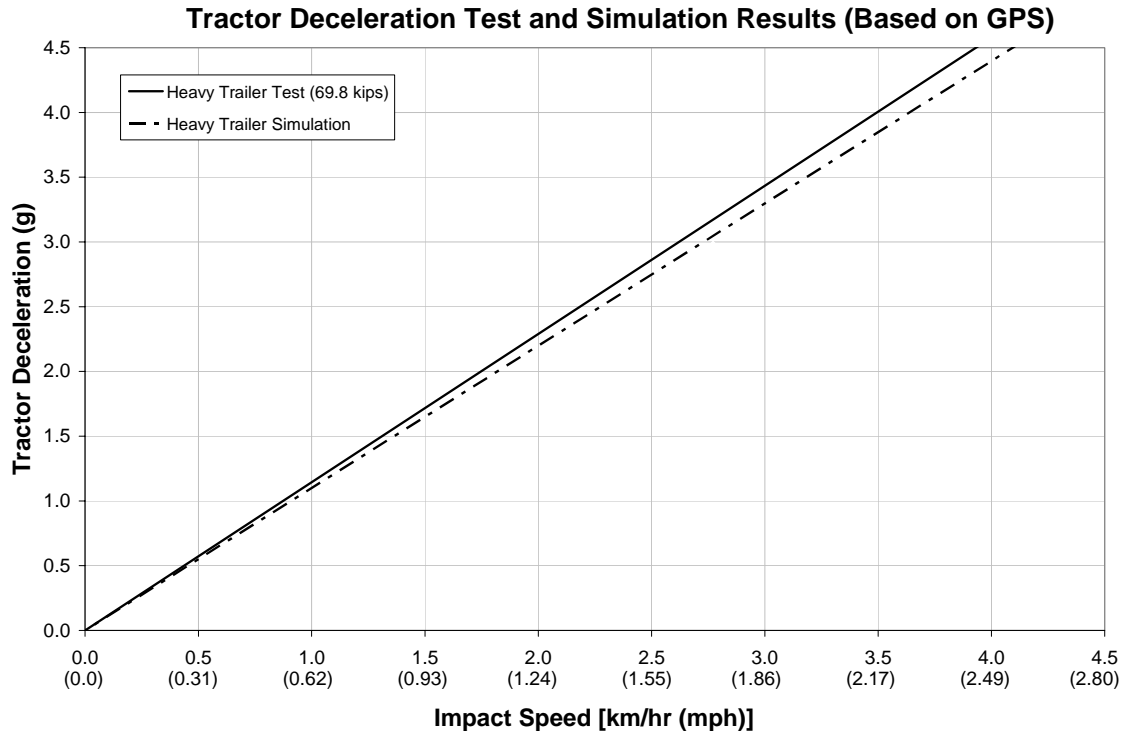


Figure 4.5: Mack Trucks simulated and measured tractor deceleration vs. impact speed (GPS)

The test data and simulation results demonstrate that the tractor deceleration increases linearly with impact speed, as expected. The simulated tractor decelerations and test decelerations are very close.

4.3.2 Kingpin Impact Force

The impact force was measured using an experimental force sensing fifthwheel provided by SAF-Holland. Data is recorded for forces on the left and right support pins attached to the fifthwheel brackets. The peak values from each time series for both the left and right pin were summed to get the total impact force.

When the force data was inspected, it was found that a larger than expected force is recorded in the vertical direction. The fifthwheel has no vertical load, so it is suspected

the wedging action occurring during coupling causes some of the longitudinal impact force to be recorded in the vertical direction, thus a fraction (0.7) of the recorded vertical forces were added to the simulated longitudinal forces to compensate for wedging.

Figure 4.6 shows the measured and the corrected predicted impact force with respect to the impact speed (GPS). The impact force increases linearly with impact speed.

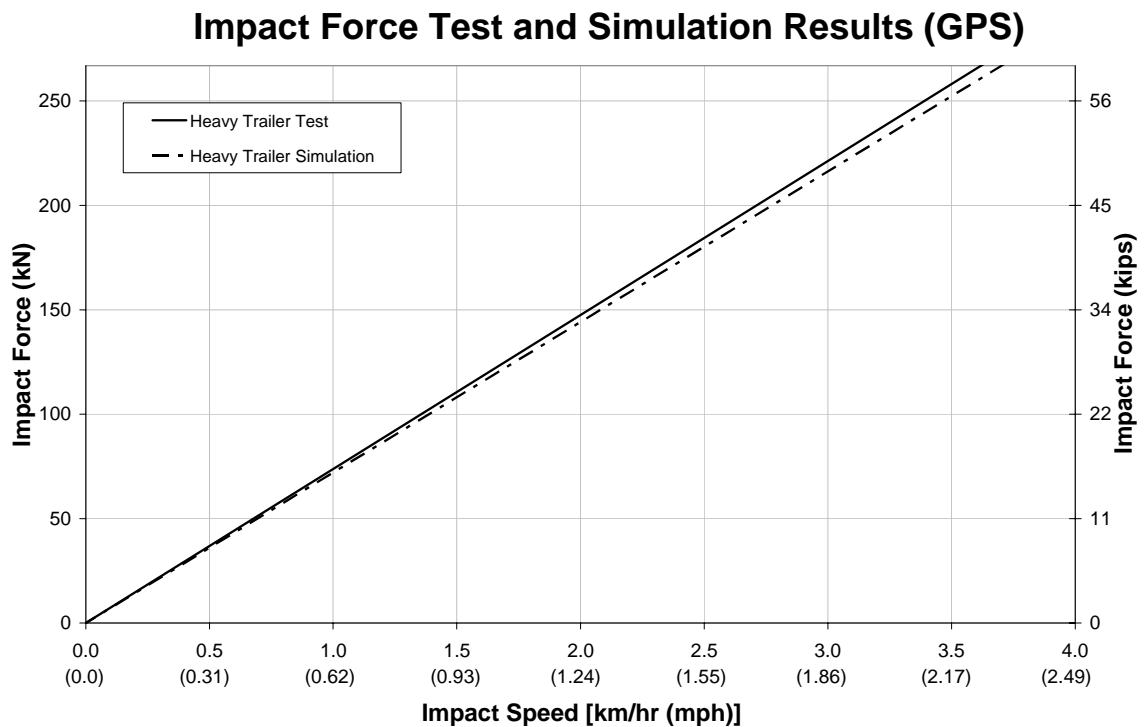


Figure 4.6: Mack Trucks measured and simulated impact force vs. impact speed

4.4 Analysis of Fifthwheel Damping System

Two types of coupling simulations are conducted to investigate the effect of a fifthwheel damping device. First, for contact force reference, the fifthwheel is restricted to only rotation about the bracket pivot joint. This “fixed” coupling simulation is used as the baseline to compare loads transmitted to the kingpin in “sliding” bracket simulations. In

the second type of coupling simulation, the fifthwheel is free to rotate about the bracket pivot joint and the bracket was free to translate in the longitudinal direction with respect to the tractor chassis. A translational spring/damper joint was implemented in the longitudinal direction between the fifthwheel brackets and the tractor chassis. This translational spring/damper joint allowed the impact load transferred from kingpin to fifthwheel to be significantly reduced. For the sliding bracket, two different spring stiffnesses were simulated using a constant damping coefficient. The objective was to predict the optimal damping system that may be used for the reduction of the kingpin impact force for this specific vehicle configuration.

An optimal damping system would reduce the tractor deceleration and impact force on the kingpin while maintaining minimum bracket displacement. The simulations were run with a fixed-bracket baseline, a 1.4 kN/mm spring, and a 2.8 kN/mm spring. Both damping systems used a 5 N-s/mm damper. From the simulations performed, an optimum damping system was selected.

Figure 4.7 shows the simulated impact forces during coupling using the damping system concept. The heavy (310.5 kN, 69.8 kips) and light (105.9 kN, 23.8 kips) trailer weights were plotted together for each spring/damper design to show the effect of weight on the damping system's performance.

Figure 4.8 shows the simulated tractor decelerations during coupling using a fixed bracket and two different spring/damper systems. Two different trailer weights were plotted together for each spring/damper design to show the effect of weight on the damping system's performance.

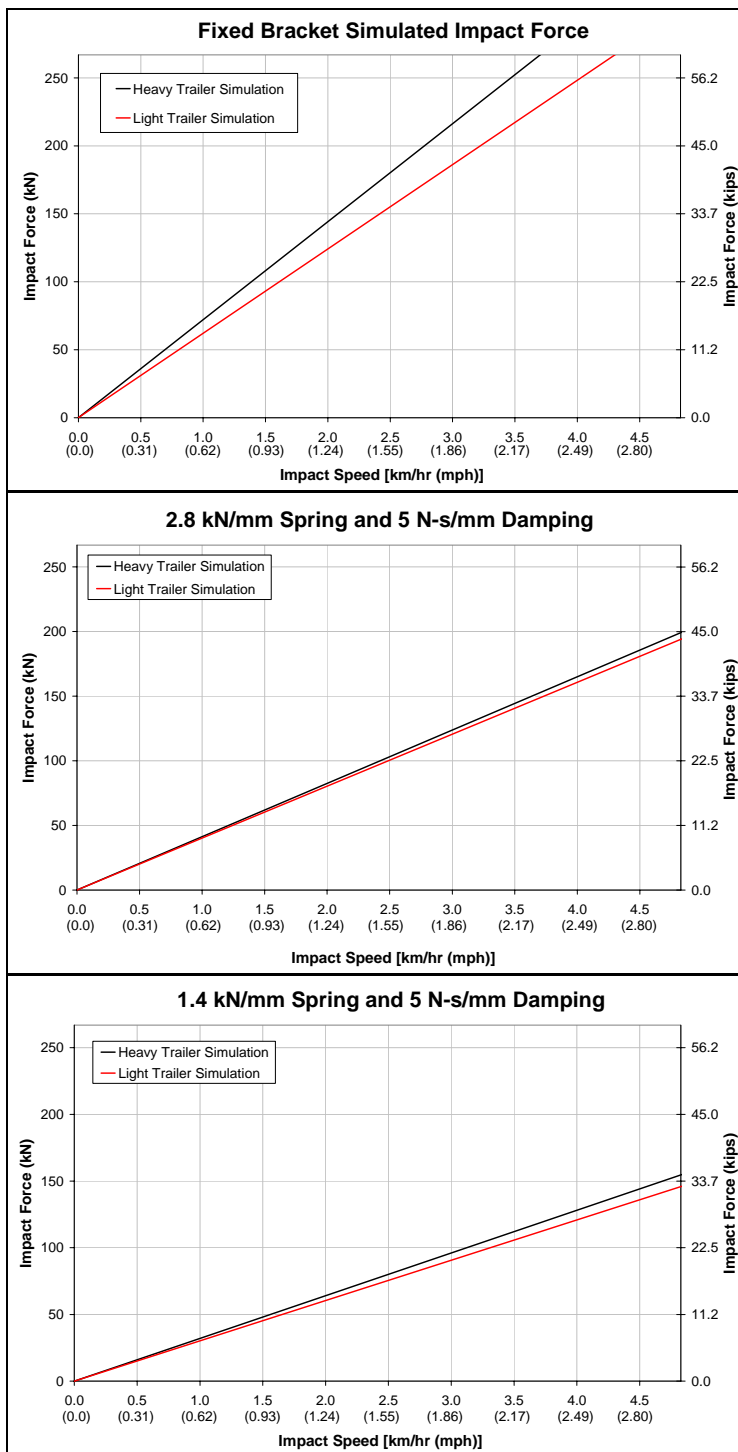


Figure 4.7: Coupling impact forces

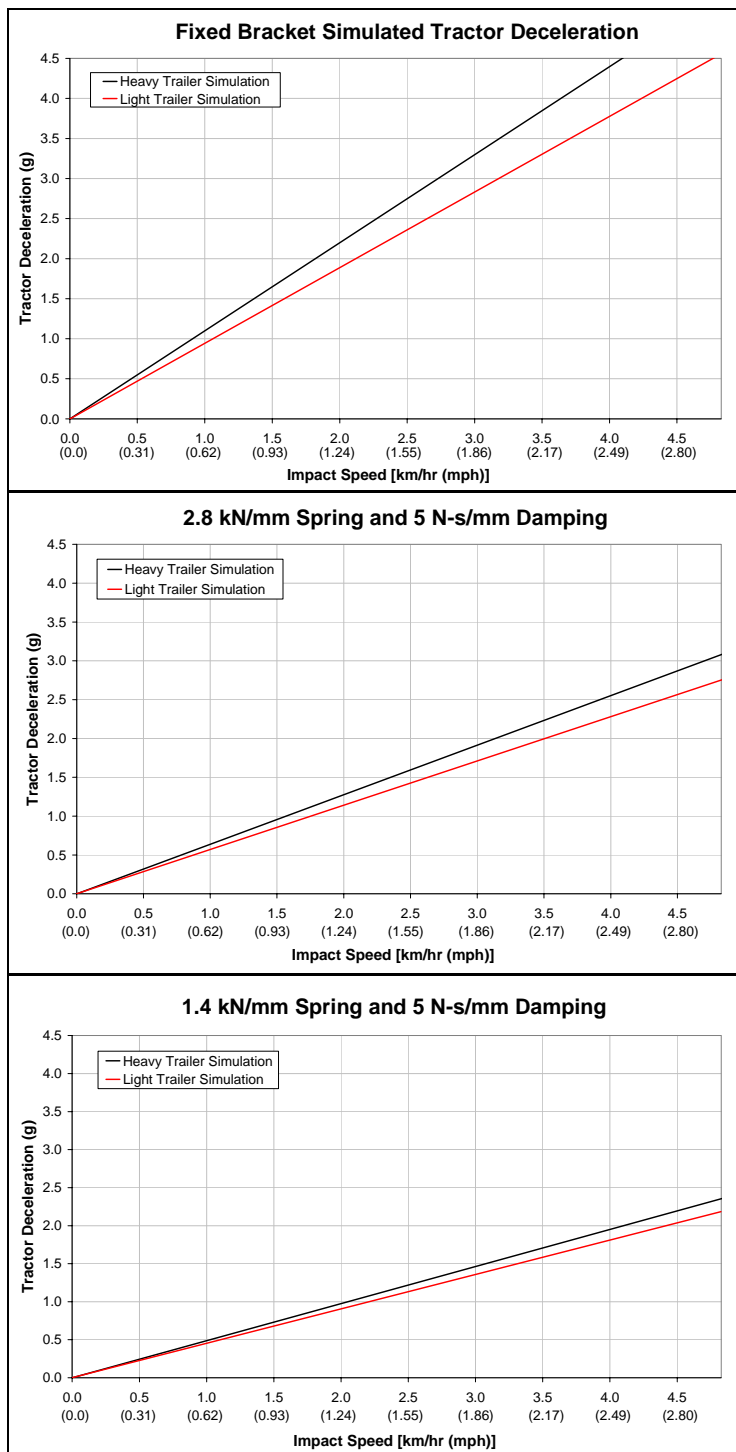


Figure 4.8: Coupling tractor decelerations

Tractor decelerations and impact forces incurred at 2 mph (3.22 km/hr) impact speeds were compiled, and using the fixed bracket as 100% tractor deceleration and impact force, the percent reduction created by each damping system was tabulated in Table 4.3.

Table 4.3: Percent reductions by damping system

	Heavy Trailer		Light Trailer	
	2.8 kN/mm	1.4 kN/mm	2.8 kN/mm	1.4 kN/mm
Spring Constant:				
Tractor Deceleration Reduction:	41.1 %	55.4 %	41.8 %	53.3 %
Impact Force Reduction:	41.5 %	54.9 %	35.9 %	54.0 %

Figure 4.9 and 4.10 show the bracket displacement (i.e., the maximum extended length of the spring/damper between the tractor chassis and the bracket) during coupling for both simulated trailer weights. The softer (1.4 kN/mm) spring and the stiffer (2.8 kN/mm) spring were plotted together for each semitrailer weight case. The two graphs for the heavy and light trailers are quite similar. This implies that the bracket displacement of the damping system is not dependent on the trailer weight.

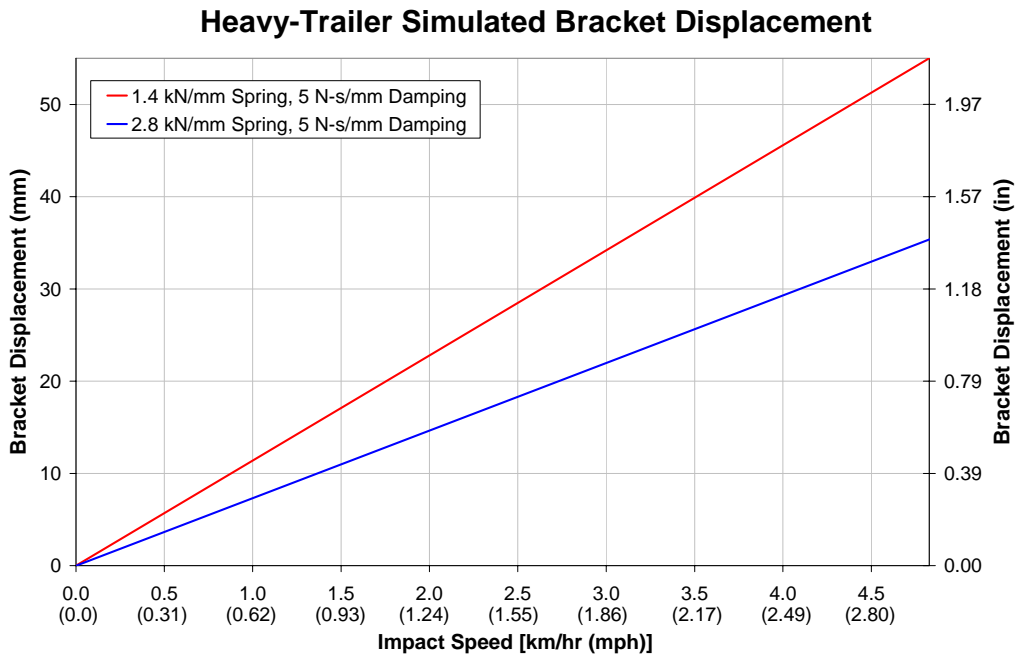


Figure 4.9: Bracket displacement during heavyweight semitrailer coupling

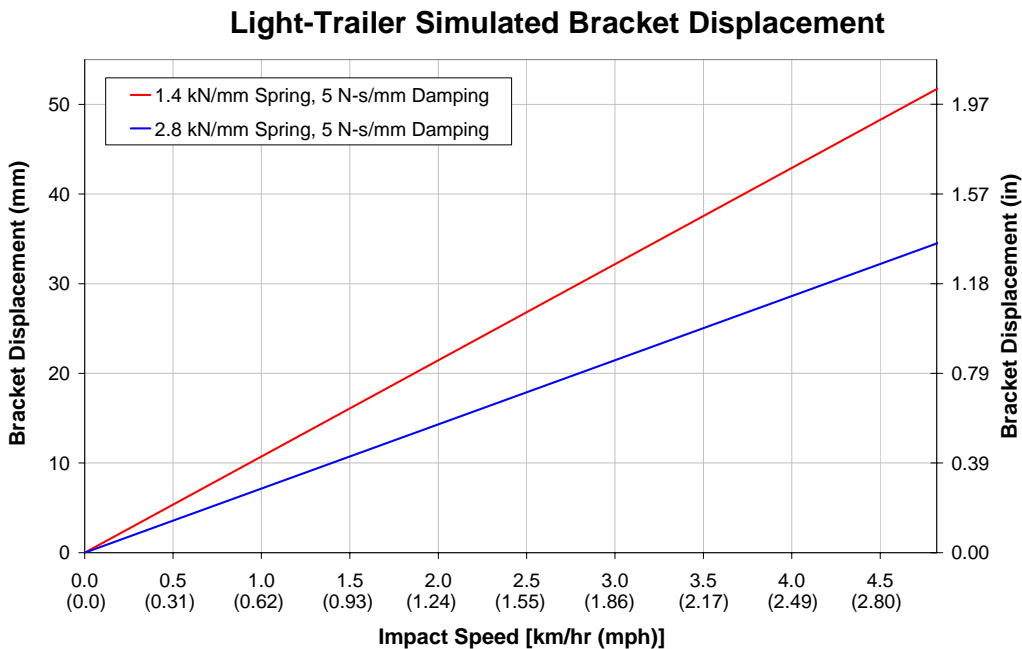


Figure 4.10: Bracket displacement during lightweight semitrailer coupling

Chapter 5

ELASTIC KINGPIN SUPPORTING STRUCTURE

In this chapter, the current fully developed Mack Trucks coupling model is used to further investigate the effects of kingpin load on the kingpin supporting structure. The “Heavy” trailer from previous simulations was used. The mass properties of the new elastic kingpin supporting structure model can be seen in Table 5.1.

Table 5.1: Mass properties of tractor and semitrailer

	Weight
Tractor	64.90 kN (14.590 kips)
Heavy Trailer	310.5 kN (69.803 kips)

The Mack Trucks tractor and semitrailer were copied from the previous models described previously, but the semitrailer FEA mesh was changed for the analyses in this section.

5.1 Model Construction of Elastic Kingpin Supporting Structure

The entire supporting structure above and around the kingpin was modeled using elastic shell elements. A shell element effectively models these relative thin parts very effectively in the FEA code while using less computational time when compared with an elastic solid element. Specifically, a linear elastic isotropic thin shell continuum material model was used to model the supporting structure parts. The elastic behavior of this material is governed by the elastic modulus (E), the shear modulus (G), Poisson’s ratio (ν), and thickness (t) [13]. The steel structure material properties are shown in Table 5.2.

Table 5.2: Material parameters used for steel

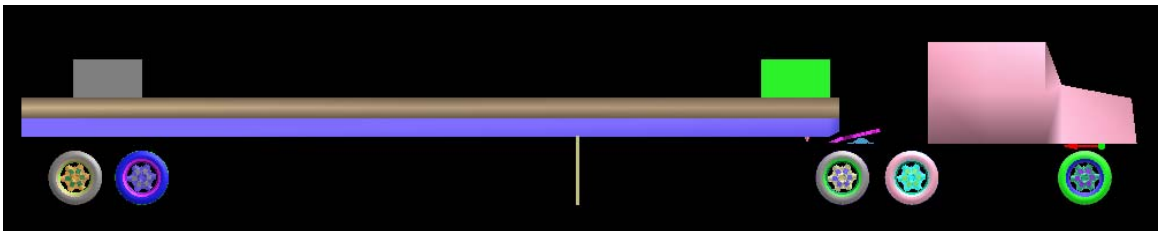
Elastic Modulus (E)	200 GPa
Shear Modulus (G)	76.9 GPa
Poisson's Ratio (ν)	0.3

The supporting structure consists of six elastic parts, and the kingpin is modeled a rigid entity. The thicknesses of the elastic parts are shown in Table 5.3.

Table 5.3: Thickness of selected parts in FEA model

	Thickness [mm (in)]
Bolster Plate	6.35 (0.250)
Left C-Beams	4.76 (0.187)
Right C-Beams	4.76 (0.187)
Center Support	11.12 (0.438)
Front Lateral Support	4.76 (0.187)
Rear Lateral Support	4.76 (0.187)

Figure 5.1 shows the entire side view of the model. This model is identical to the Mack Trucks model with the heavy trailer. The weights of the tractor-semitrailer system are listed above in Table 5.1.

**Figure 5.1: Entire side view of elastic kingpin structure model**

A close look at the supporting structure will provide a better understanding of how the model was assembled. Figure 5.2 shows a bottom view of the semitrailer. This view

offers a good look at how the kingpin and supporting structure is attached to the trailer main beams.

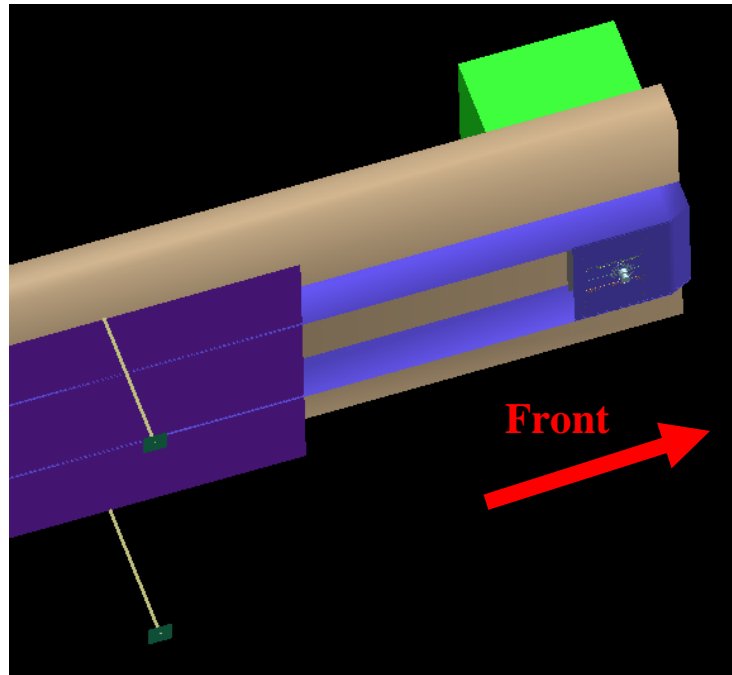


Figure 5.2: Bottom isometric view of semitrailer

Figure 5.3 is a screenshot that shows a bottom view of the bolster plate finite element mesh while attached to the trailer. As indicated in the bottom view, the shell elements extend radially from the centrally located kingpin.

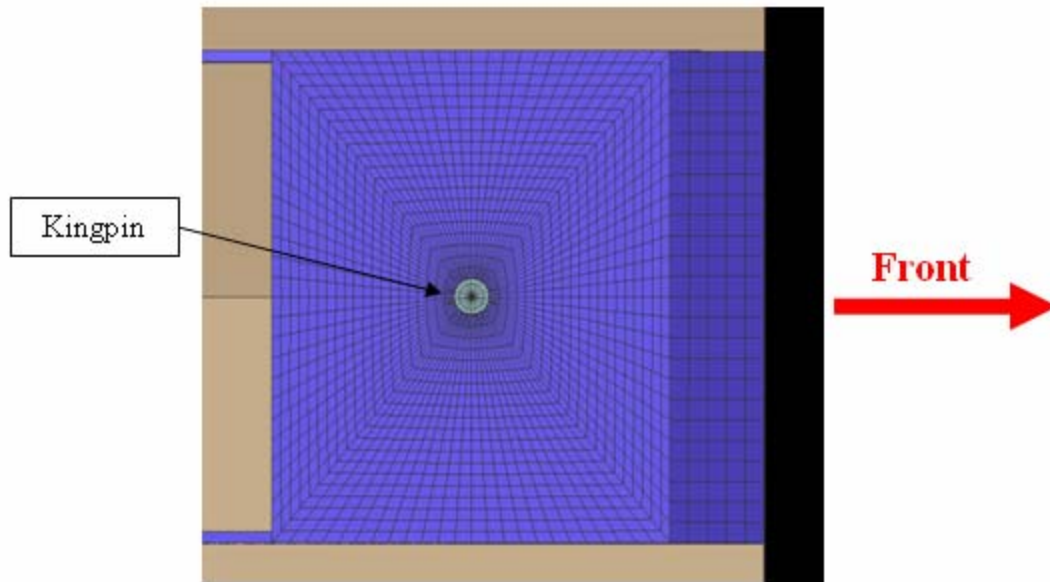


Figure 5.3: Bottom view of bolster plate

Figure 5.4 is an isometric view of the top of the kingpin support structure. All of the other parts from the semitrailer have been removed to allow a better view of the support structure mesh. The bolster plate is the bottom plate that contacts the top of the fifthwheel during normal operation of the tractor-semitrailer. The front and rear lateral supports are steel C-channels that runs between the two main beams of the semitrailer. The center support is a thick steel plate that is welded across the top of the kingpin and runs between the front and rear lateral supports. Lastly, the right and left C-beams run parallel to the center support between the front and rear lateral supports.

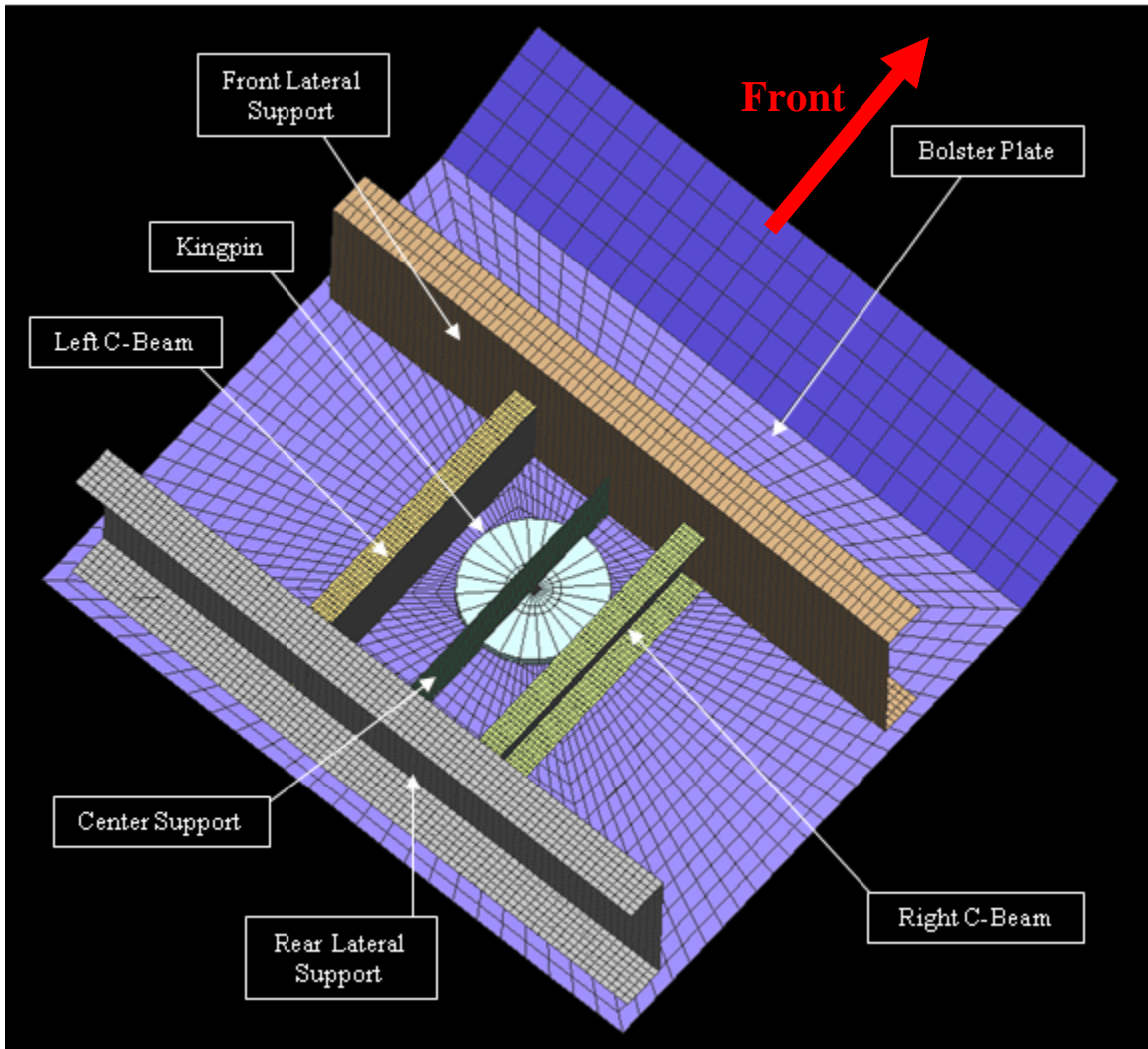


Figure 5.4: Labeled isometric top view of the kingpin and support structure

The structure is attached to the rest of the rigid semitrailer parts by defining rigid nodes around the outside edge of the bolster plate and along the right and left edges of the lateral supports. Because the elastic parts are not rigidly connected, a Pam-Crash weld model was used. The weld points are used to define attachment points between parts with an elastic material definition. Each weld point is defined by a position relative to each part and the parts it is connecting. A total of 377 weld points are used in this model. Figure 5.5 shows an isometric top view of the kingpin and supporting structure with the weld points displayed in red.

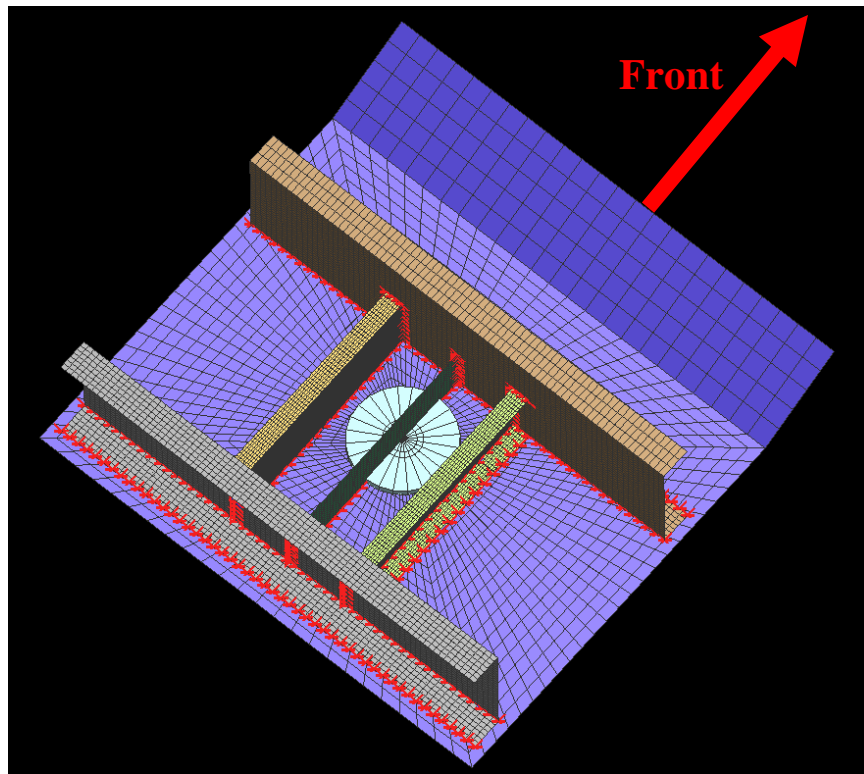


Figure 5.5: Isometric top view of kingpin supporting structure with weld points

Figure 5.6 is a closer view of the supporting structure with the rear lateral support and right C-beam removed. This allows a better view of the center support and the lateral support structure mesh. The weld points are still visible, but it can be noticed that the top of the kingpin is not welded to the center support. Because the kingpin is a rigid body, the nodes of the center support that border the kingpin are defined in the rigid body card of the kingpin.

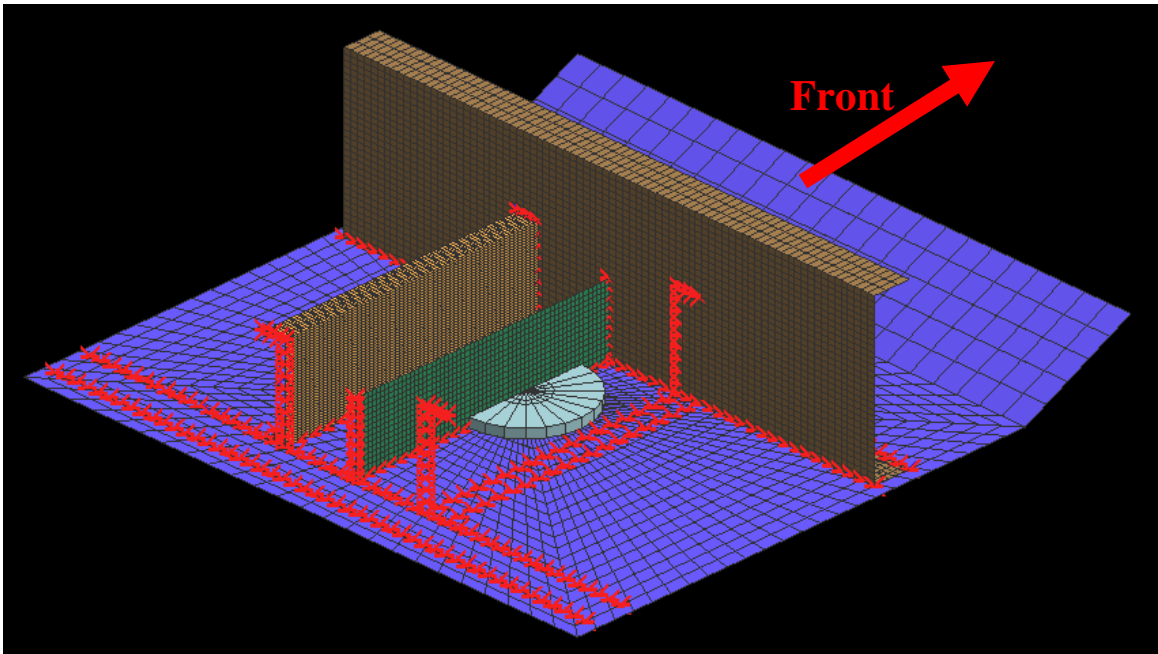


Figure 5.6: Cut-away view of the kingpin support structure and weld points

5.2 Validation of Elastic Kingpin Supporting Structure Model

The model containing an elastic kingpin supporting structure was compared to the Mack Trucks model and the Mack Trucks measurements for validation. This section will compare the kingpin impact force and tractor decelerations between models.

First, the impact force was plotted with respect to impact speed on the same graph as the Mack Trucks model validation. Figure 5.7 shows the data from the elastic kingpin support structure simulation with the Mack Trucks model and experimental test results. The impact forces extracted from the elastic kingpin support structure simulation are very similar to those of the original Mack Trucks model. The impact forces from the elastic structure simulation are slightly lower than the Mack Trucks model outputs; there is a maximum 3% difference in kingpin impact forces predicted using the elastic kingpin support structure and the original Mack Trucks coupling model.

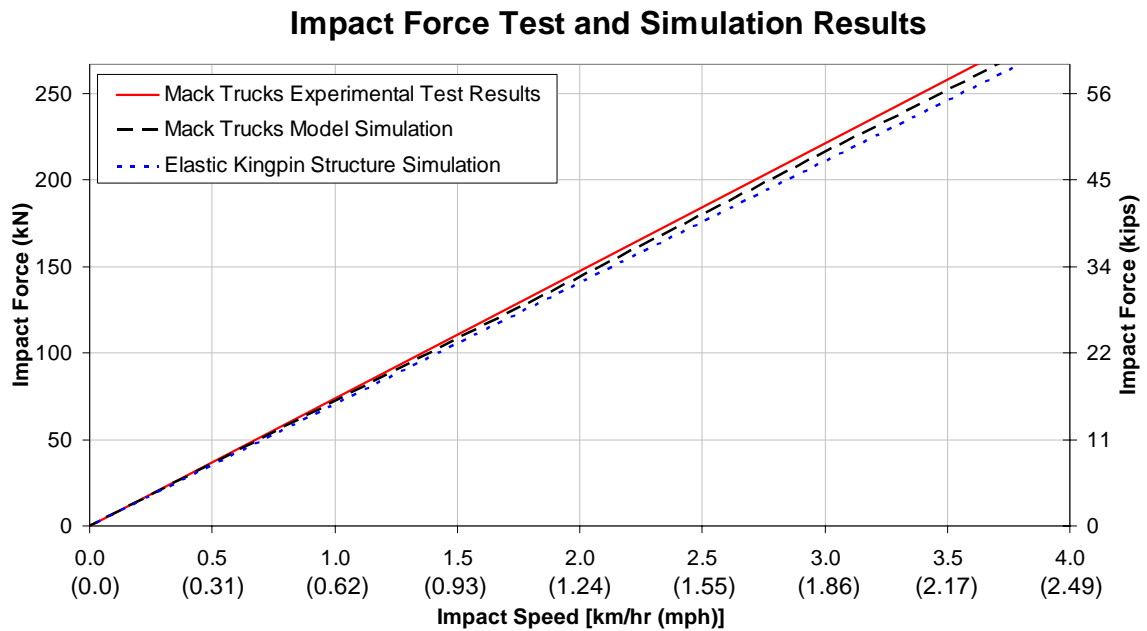


Figure 5.7: Kingpin impact force vs. impact speed for validation of elastic model

Next, the tractor deceleration data was plotted as a function of impact speed. The elastic kingpin structure's tractor deceleration data is shown in Figure 5.8 along with both the Mack Trucks model output and measured experimental test results. The elastic kingpin support structure simulations show output deceleration values within 2.6% of the tractor decelerations provided by the original Mack Trucks model.

Both the impact force and tractor deceleration data sets are shown to be very similar to those calculated using the Mack Trucks model. The trends shown in Figure 5.7 and Figure 5.8 are extremely comparable to one another, and thus the elastic kingpin support structure is shown to have a limited effect on the coupling behavior of the system.

The stresses within the elastic elements were not extracted from these coupling simulations. The impact occurs too quickly for the output frequency to provide an accurate result across the entire time interval of the coupling simulation. The following simulations employ a constant force on the kingpin and allow a consistent stress distribution to be captured using the FEA model.

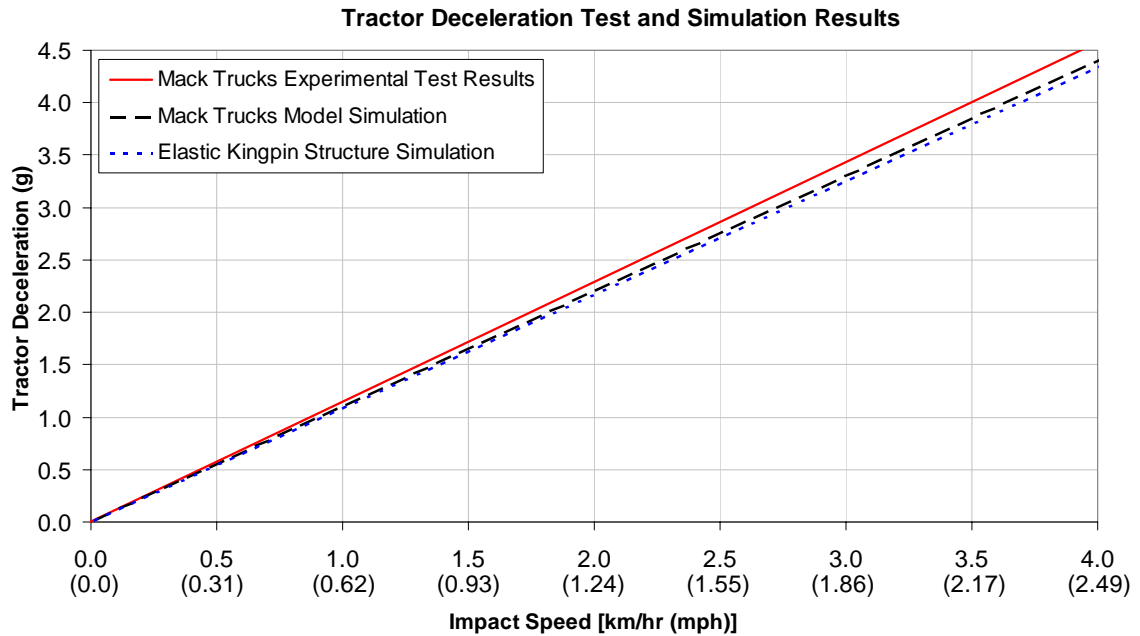


Figure 5.8: Tractor deceleration vs. impact speed for validation of elastic model

5.3 Simulations of SAE J133 loads “A” and “E”

Using the validated elastic kingpin support structure model, the loads “A” and “E” will be modeled as defined by SAE Standard J133. These simulations will provide approximate stress distributions in the elastic support structure produced by the SAE prescribed loads applied to the kingpin.

The horizontal load “A” is modeled using two simulations. The first models the force in the location defined by the current SAE J133, and the second simulation uses the force location defined in Figure 1.4. The difference between the two point loads is clearly illustrated in Figure 1.4. For the Mack Trucks heavy trailer, load “A” was calculated to be 357.08 kN (80.27 kips).

The SAE specified load application point was simulated and the resulting Von Mises Stress contour plot is shown in Figure 5.9 and Figure 5.10. The rear lateral support and right C-beam have been removed for a better view of the structural parts that are being strained.

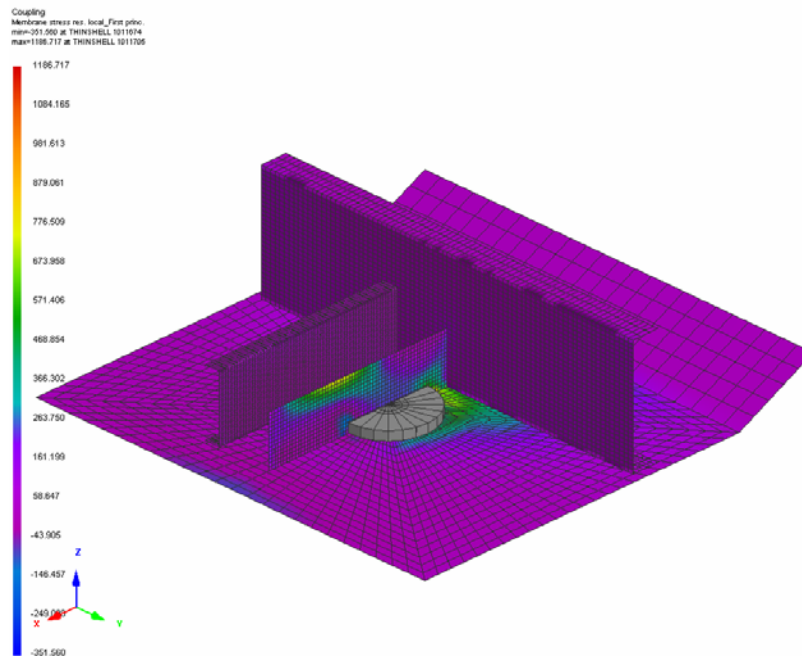


Figure 5.9: Isometric view of current SAE J133 load “A” Von Mises stress plot

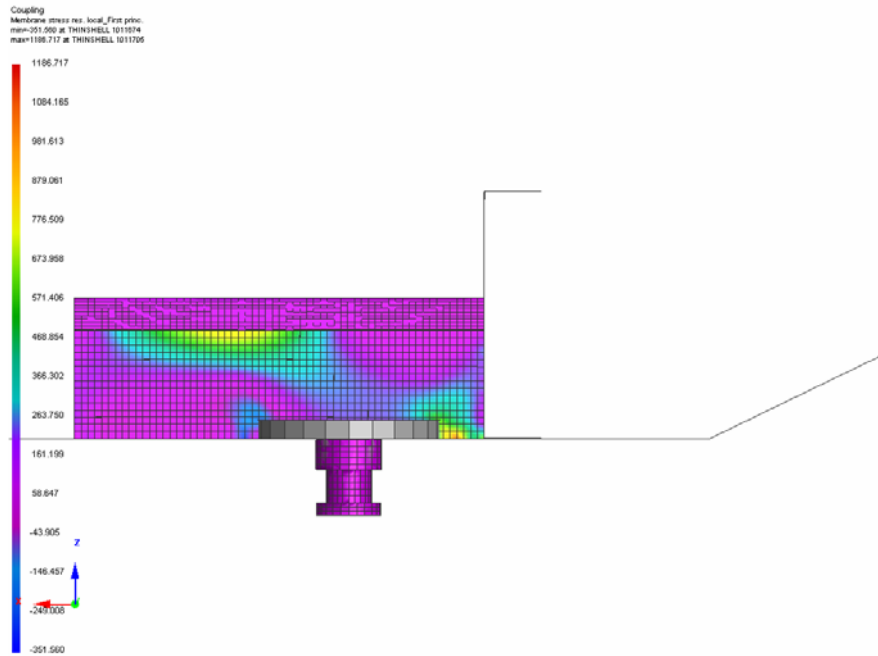


Figure 5.10: Side view of current SAE J133 Load “A” Von Mises stress plot

When the load is correctly applied to the kingpin, the moment transferred to the support structure is increased. Figure 5.11 shows the isometric view of the Von Mises stress contour plot showing the first principle stress. Figure 5.12 shows the side view of the Von Mises stress contour. This view shows the center support carrying a large portion of the load.

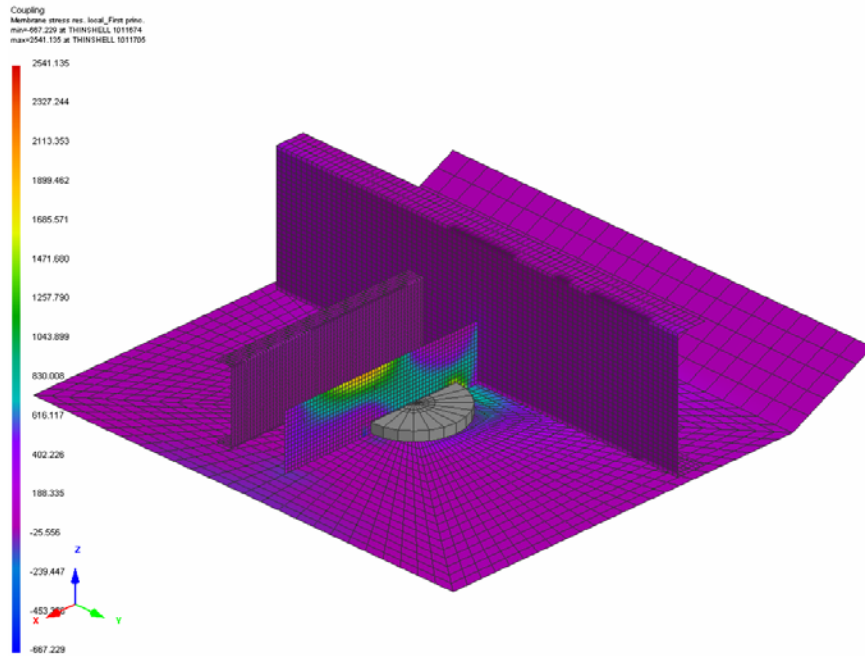


Figure 5.11: Isometric view of corrected SAE J133 load “A” Von Mises stress plot

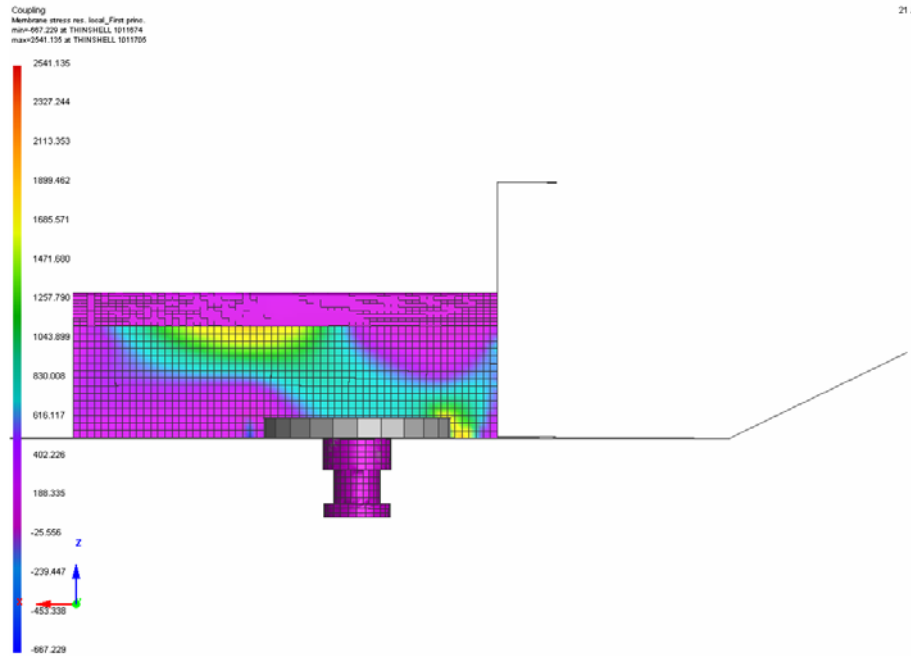


Figure 5.12: Side view of corrected SAE J133 load “A” Von Mises stress plot

The two simulations of point load “A” provide similar distributions of stress, but the correctly applied load induces a much higher value of stress. This adverse effect is due to the increased moment arm that is presented to the system when the load is moved. The moment causes higher stress values at the front point of the kingpin and translates to the rear of the center support and on throughout the rest of the structure.

The vertical load “E” is modeled using two simulations: one simulation is conducted with the force acting on the kingpin in the downward direction and the other with the force in the upward direction. For the heavy Mack Trucks test trailer, the calculated load “E” is 310.5 kN (69.8 kips). Figure 5.13 shows the Von Mises stress contour plot of the downward load “E” from an isometric view.

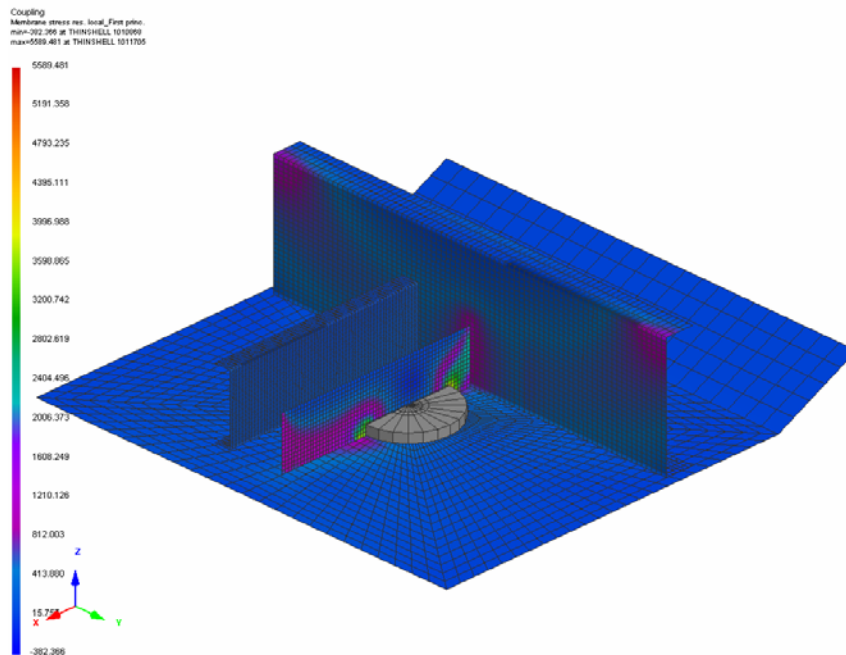


Figure 5.13: Isometric view of Von Mises stress plot from the downward load “E”

Figure 5.14 shows the same downward application of load “E” but with a side view of the center support.

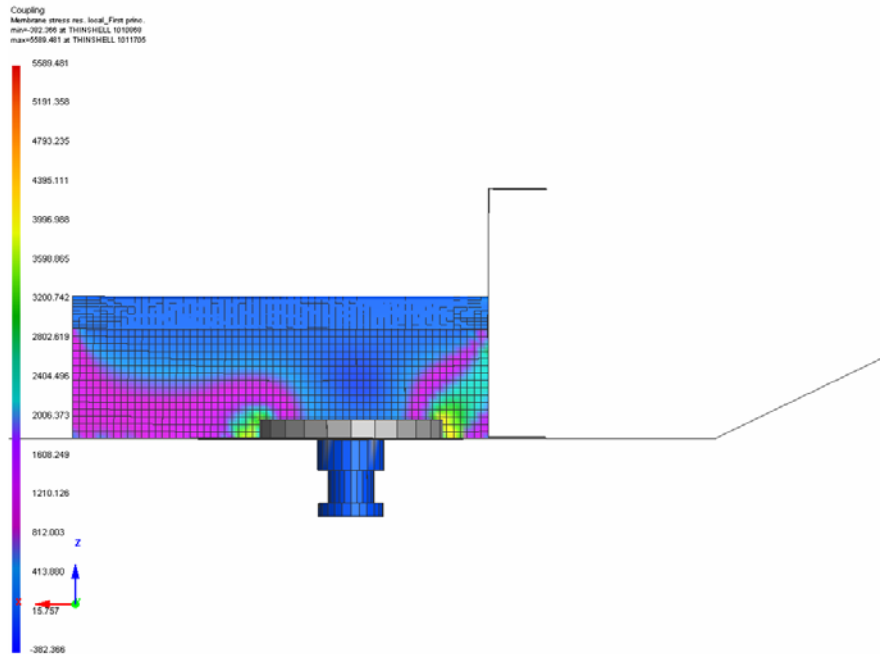


Figure 5.14: Side view of Von Mises stress plot from the downward load “E”

Figure 5.15 and Figure 5.16 show the Von Mises stress contour plots from the upward simulation of SAE J133 load “E”.

A higher magnitude of compressive stress is seen in the downward force of load “E”, but a greater tensile stress is observed in the upward direction. This can be misleading because in operation the upward force on the semitrailer is transferred through the entire contact plate by the fifthwheel. Force “E” from the SAE Standard J133 is meant to be a one-time application of a vertical test load to verify acceptable kingpin installation. The upward simulation of this force is included in this research for comparison purposes.

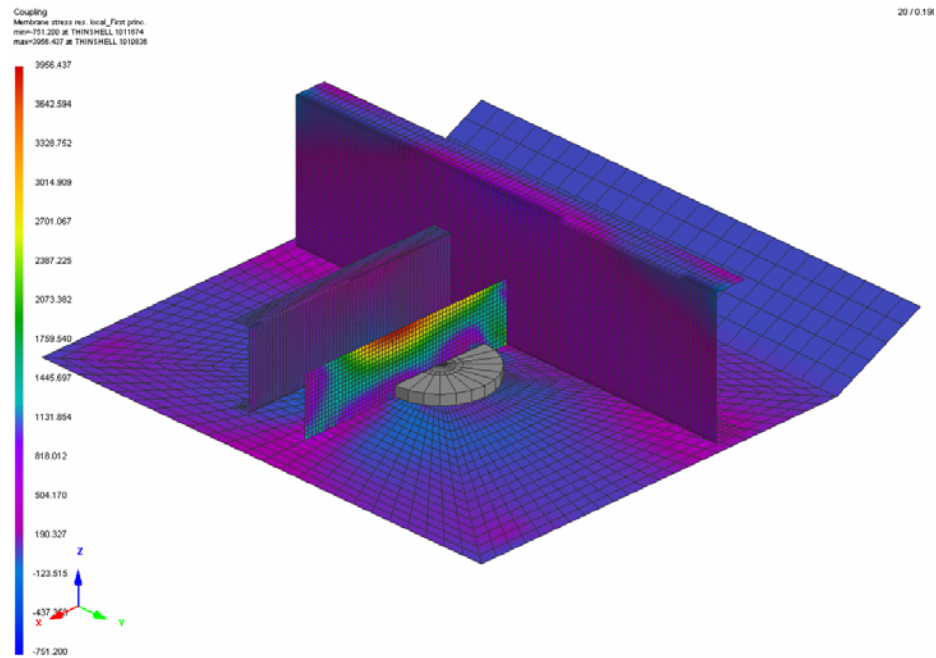


Figure 5.15: Isometric view of Von Mises stress plot from the upward load “E”

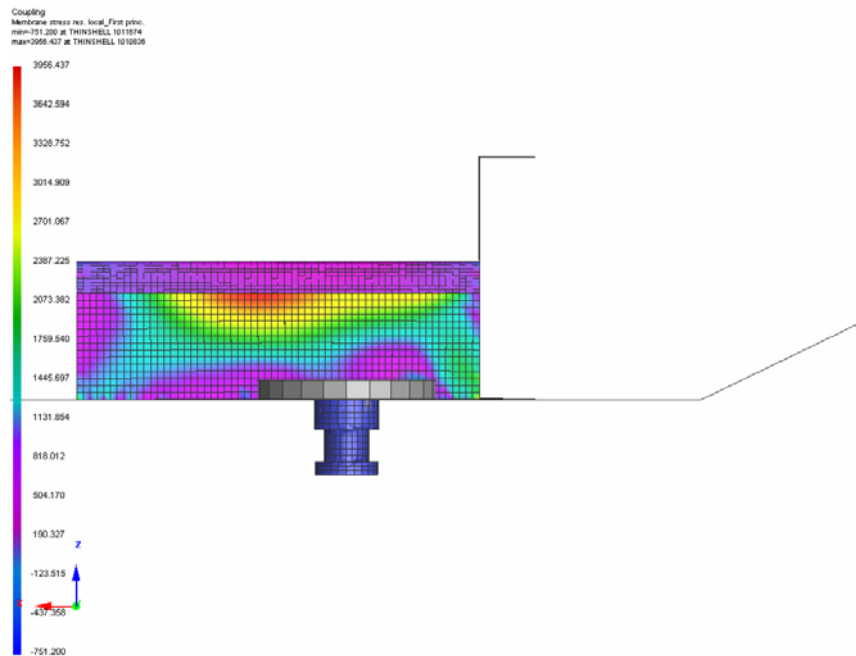


Figure 5.16: Side view of Von Mises stress plot from the upward load “E”

Chapter 6

CONCLUSIONS AND RECOMMENDATIONS

Three coupling finite element models were created for the research in this thesis: one model was used to simulate the coupling tests performed by ARL, the second model was used for Mack Trucks coupling test simulations, and the last model was used to analyze the steel kingpin support structure of Mack Trucks' semitrailer.

In the literature review, it was found that the SAE standard J133 contains obscure drawings and incorrect descriptions. SAE J133 defines a force "E" and gives a calculation of the force, but the figure showing the location of force "E" is missing from the standard. Also, the load application points of the standard's defined loads "A" and "B" are incorrect. Some of the most important findings of this study are the problems found within the published SAE J133.

In general, the FEA models in their final form have been shown to closely predict tractor CG decelerations at impact between the kingpin and fifthwheel during coupling. This has been validated with experimental data from both the ARL tests and the Mack Trucks tests. When using the experimental data from the SAF-Holland fifthwheel, it has been shown that the loads at the kingpin and fifthwheel during coupling coincide with the output from the FEA models. Computer Aided Engineering (CAE) can be used to accurately predict the kingpin impact loads for all three models developed.

6.1 ARL Coupling Tests

Using the experimental deceleration data collected from the tests, a FEA model was developed using Pam-Crash Systems and validated to within 33% accuracy. The tractor's deceleration was found to increase linearly with coupling impact speed.

The ARL coupling model was designed for easy extraction of the following data:

- Tractor velocity
- Tractor and semitrailer accelerations
- Contact force at the kingpin and fifthwheel interface
- Mass properties for weight distribution analysis
- Longitudinal damping system bracket displacement

The tests completed at ARL facilities were planned and conducted very well. A selection of three impact speeds was tested from approximately 1 km/hr (0.62 mph) to 5 km/hr (3.11 mph). Measurement of relatively slow speeds such as these posed a large problem. The low speed measurement system was composed of a tachometer coupled to the tractor's driveline. This worked very well at measuring the low speeds exhibited during the coupling maneuvers.

Further simulations were conducted to analyze the effect of trailer weight on tractor deceleration. A simulation was performed using the validated ARL tractor and semitrailer model, but the trailer mass was increased significantly. The simulation predicted that semitrailer weight has a direct effect on the impact force and tractor deceleration during coupling. In conclusion, the ARL coupling tests were successful in validating tractor decelerations at various coupling impact speeds.

6.2 Mack Trucks Coupling Tests

The coupling experiments conducted at Mack Trucks were quite unique. This was the first time that an instrumented fifthwheel was ever used to measure kingpin impact forces during coupling. These tests provided interesting insight into the dynamics of a tractor/semitrailer system during such an operation.

The Mack Trucks coupling model was similar to the ARL model in that much of the same data was easily obtained from the model outputs. The Mack Trucks model was designed to easily obtain the following predicted data:

- Tractor velocity
- Tractor and semitrailer accelerations
- Contact force at the kingpin and fifthwheel interface
- Two mass boxes on the trailer for simple weight distribution manipulation
- Longitudinal damping system bracket displacement

The Mack Trucks FEA model created for this research was shown to predict tractor CG decelerations for a heavy weight trailer to within 10% accuracy. The trends of the measured impact forces follow those of the measured decelerations. The simulated and measured kingpin impact forces for the heavy weight trailer are in good agreement with each other.

The method of measuring impact speed during the Mack Trucks experimental tests was not as effective as the method employed during the ARL tests. It was found that the refresh rate of the GPS was very slow, and the digital video contained too much inherent error when trying to measure an instantaneous speed. Several improvements could be made to improve the accuracy and consistency of the speed measurements during these tests.

Because Holland's instrumented fifthwheel had never been used to measure coupling forces, much was learned from conducting the coupling experiments. From what was observed during the coupling tests at Mack Trucks' facility, several improvements could be made. Also, work must be done to understand how to use this instrument for impact testing.

Much data was obtained from the Mack Trucks coupling tests. Various impact speeds were recorded for two different semitrailer weights. Variation in test data was caused by

numerous factors. Due to experience, a driver's natural tendency is to apply the brakes before contacting the kingpin during coupling. While conducting the tests, this was apparent. It was also noticed that as impact speed was increased the application of brakes had more of an effect on the recorded data. The braking during coupling would lower the impact speed, making it more difficult to extract the true impact speed from the data. Also, the braking would decrease the true kingpin impact force and tractor deceleration from coupling.

Another factor in test data variation was the sliding of the trailer wheels during coupling. During testing, both trailers had their brakes locked to keep the wheels from rolling. This is common for coupling maneuvers. For impact tests, deceleration and force measurements require a solid base. It was observed that the lightweight trailer tires slid several inches on the road surface. This would result in lower deceleration and impact forces. The data confirmed this.

The last factor that significantly affected the data was the kingpin impact angle. In addition to a solid impact surface, the semitrailer's kingpin must be impacted squarely, without any scrubbing action when entering the fifthwheel slot. If the kingpin strikes or glances off the fifthwheel, a reduction in deceleration and forces will result. During testing of the lightweight trailer, the kingpin was seen scrubbing against the side of the fifthwheel slot. This would lower the predicted deceleration and impact force values when compared to ideal conditions.

6.3 Fifthwheel Damping System Analysis

The fifthwheel damping device originated as a method to reduce kingpin impact force as well as tractor deceleration. This is exactly the results that were obtained from simulations of this device. Structurally, the kingpin and the kingpin support structure on the semitrailer should not be subjected to the extreme loads exhibited during coupling. Also, the driver experiences a large shock and subsequent discomfort from the impact

deceleration of the tractor during coupling. The translational fifthwheel spring/damper system showed considerable reduction of impact force and tractor deceleration.

The original analysis was performed using the validated ARL model. A simple sensitivity analysis was conducted in which the parameters of the damping device were selected in order to decrease the kingpin impact force while maintaining an acceptable bracket displacement. From these simulations it was found that the displacement of the brackets during coupling is independent of the trailer load. The simulation and measured results have provided enough information to design a fifthwheel damping system to reduce the tractor deceleration and kingpin impact force. The simulations have provided a set of parameters that is specific to the tractor/semitrailer system selected for this research.

6.4 Elastic Kingpin Supporting Structure Model

The elastic kingpin supporting structure model was validated using the Mack Trucks model validation data. The elastic kingpin supporting structure model was within 3% for both the kingpin impact force and the tractor deceleration when compared with the original Mack Trucks coupling model.

Both the kingpin impact force and tractor deceleration trends were quite similar and linear in trend, but the elastic structure provided slightly lower values than the rigid structural model. This supports the idea that the energy is being absorbed by the tires, suspensions, and long structural members used to create a long wheelbase for the semitrailer. The kingpin support structure was shown to act more as a rigid entity when comparing the tractor/semitrailer systems; however, the stress distributions within the center support of the support structure indicated concentrated areas of stress that could lead to failure.

The elastic kingpin supporting structure model took an extremely large amount of computational time. The original Mack Trucks coupling model was on the order of fifteen times more time efficient.

6.5 Recommendations

The research for this thesis resulted in a few recommendations. First, this study recommends full revision of SAE Recommended Practice J133 to correct several serious mistakes. The mistakes to be corrected include fixing incorrect placement of forces in diagrams, justification of forces' limits, developing ineffective test fixtures, and providing missing or poor sketches. Also, it is recommended that an SAE standard be developed for the installation of kingpins. During the investigation of kingpin loads, it was found that the lack of a standard for kingpin installation has resulted in inadequate kingpin support structures.

Also, it is recommended that the Mack Trucks coupling tests be run again in order to provide more accurate results. The low speed measurement system needs to be reevaluated—the GPS and digital video methods provided poor speed measurements. A method of measurement such as a string pot sensor or a tachometer/driveline system such as the one employed in the ARL tests should be used. In addition, a method of running the tests should be developed in order to decrease driver error. This includes actions such as misapplication of brakes and off-angle impacts of the kingpin on the sides of the fifthwheel.

Lastly, it is recommended that a prototype translational damping system be built and tested using a calibrated force-measuring fifthwheel. This could be used to determine its suitability for kingpin load reduction during typical tractor-semitrailer operations. If possible, the validation tests of the translational sliding fifthwheel damping system should be conducted in collaboration with Mack Trucks and SAF-Holland.

BIBLIOGRAPHY

1. Shoffner, B., Allen II, J., El-Gindy, M., Evenson, W., Scaglione, M. "Prediction of Kingpin/Fifthwheel Forces for Tractor-Semitrailers During Typical Operating Maneuvers", 2007 ASME International Design Engineering Conferences, 9th International Conference on Advanced Vehicle and Tire Technologies (AVTT), Las Vegas, Nevada, September 4-7, 2007.
2. SAE J133, "Fifthwheel Kingpin Performance – Commercial Trailers and Semitrailers", SAE Recommended Practice, 1987.
3. ISO 8717, Commercial Road Vehicles – Fifthwheel Couplings –Strength Tests, *International Standard*, 2000.
4. SAE J700, "Upper Coupler Kingpin- Commercial Trailers and Semi Trailers", SAE Standard, 1993.
5. Cummings, S. and Koch, K., "Kingpin Load Evaluation", U.S. Department of Transportation, Federal Railroad Administration, Final Report No. DOT/VNTSC/FRA-03/06, June, 2003.
6. Sweatman P. F., "Strength Requirements for Fifthwheel Couplings in Road Trains and General Articulated Vehicles," Australian Road Research Board, Research Report ARR 149, 1987.
7. Teresinski, R. L., (1970), "Tractor-Frame-Fifth Wheel Analysis," pp. 16-23, SAE Paper # SP-354: Parameters for Proposed Fifth Wheel Coupler Installation Practice.
8. Dixon, W. G., (1970), "Practical Considerations for the Optimization of Fifth Wheel Coupler Attachment," pp. 24-34, SAE Paper # SP-354: Parameters for Proposed Fifth Wheel Coupler Installation Practice.

9. Škorjanc, J., and Ulaga, S., (1993), "Designing the Fifth Wheel Coupling Using CAD."
10. Ibrahim, I. M., (2002), "Design of a Compensating Fifth Wheel for Improving the Roll Dynamic Behavior of the Tractors and Semitrailer-trailer," SAE paper No. 2002-01-3058.
11. De Regnaucourt, R. A., "Summary and Recommendation," SAE SP-354 (Parameters for Proposed Fifthwheel Coupler Installation Practice), pp. 43-50, 1970.
12. Janeway, C. R., "A Rational Analysis of Coupling Loading of Kingpin," pp. 6-15, SAE Paper No. 700193, SP-354 (Parameters for Proposed Fifthwheel Coupler Installation Practice), 1970.
13. "PAM-CRASH/PAM-SAFE 2005 Solver Notes Manual," ESI Group, p. 230, 2005.